AD-783 552

# INVESTIGATION OF COMPOSITE COATING SYSTEMS FOR RAIN-EROSION PROTECTION

Olive G. Engel, et al

Florida Atlantic University

Prepared for:
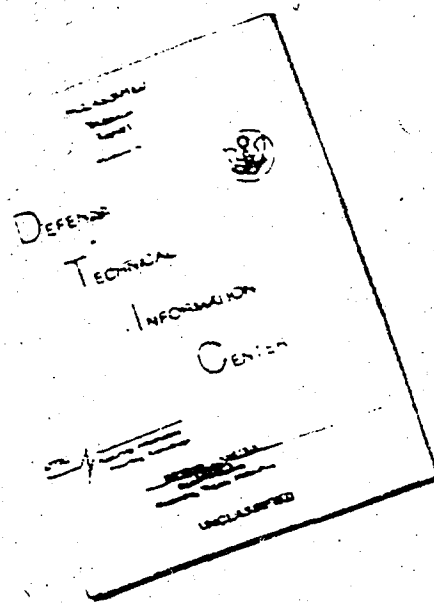
Naval Air Systems Command

15 July 1974

# DISCLAIMER NOTICE

THIS DOCUMENT IS BEST
QUALITY AVAILABLE. THE COPY
FURNISHED TO DTIC CONTAINED
A SIGNIFICANT NUMBER OF
PAGES WHICH DO NOT
REPRODUCE LEGIBLY.

INVESTIGATION OF COMPOSITE COATING SYSTEMS
FOR RAIN-EROSION PROTECTION

(15 July 1973 to 15 July 1974)


15 July 1974


by


Olive G. Engel
Department of Mechanical Engineering
and
Toyoki Nakamura
Graduate Student
Department of Ocean Engineering

for

NAVAL AIR SYSTEMS COMMAND

DEPARTMENT OF THE NAVY

by

FLORIDA ATLANTIC UNIVERSITY

BOCA RATON, FLORIDA 33432

# ABSTRACT

A further study was made of single-layer and two layer composite coatings of polyurethane. It was found that the rain-erosion resistance of both these coating types is strongly reduced by outdoor weathering in Florida for ten weeks. Both of these types of coating are strongly subject to sand erosion when sand impacts occur at normal incidence against flat test specimens. A multilayer composite coating has rain-erosion resistance equal or superior to that of a two-layer composite coating. A single-layer polyurethane softcoat may or may not have rain-erosion resistance comparable to that of a two-layer composite coating depending on the quality of the single-layer softcoat. Use of a two-layer composite coating may result in a more stable and predictable average rotating-arm lifetime than use of a single-layer coating. Although some reflection of the impact pressure pulse within a coating is beneficial, excessive reflection may be deleterious. One mode of hole formation in polyurethane coatings during rain-erosion test can be identified with formation of isolated fatigue cracks.

## TABLE OF CONTENTS

TABLE OF CONTENTS, Continued

LIST OF ILLUSTRATIONS

# 1. INTRODUCTION

The radomes and leading edges of high speed aircraft and missiles are subject to drop-impact erosion during flight through rain at low altitudes; they are subject to solid-particle impact erosion during flight through clouds of ice crystals at higher altitudes. To avert or mitigate the damage that occurs, information is needed on the impact processes and on the mechanisms of material removal and of adhesion loss associated with impingement of small masses of liquids and solids against structural materials and the coatings used to protect them.

The research described in this report is directed primarily to the high speed rain-erosion resistance of protective radome coatings. It has grown out of an investigation [1,2,3] of the relative rain-erosion resistance of two-layer composite coatings of moisture cured polyurethane materials in comparison with that of conventional single-layer coatings of these materials.

The investigation referred to was hampered by the finding that rotating-arm devices, which are currently used to test materials for rain-erosion resistance, subject rubbery coatings to at least two stresses that are not encountered on a radome during flight through rain. One of these irrelevant stresses is centrifugal force which induces fatigue cracks and loss of adhesion between coating and substrate. The second irrelevant stress is the unequal yield to which a rubbery coating applied to an acutely rounded (airfoil shaped) substrate is exposed during a drop impingement test; this stress results in fatigue cracks along the shoulder of the test specimen.

The $H_1S_2$ composite coating that was tested [2,3] is more subject to failure as a result of these irrelevant stresses than the single-layer coating. More testing needs to be done to establish with confidence whether or not a two-layer composite coating has superior rain-erosion resistance to a conventional single-layer

1.

soft rubbery coating. In addition, the relative resistance of these coating types to weathering and to sand-and-dust erosion needs to be established.

The relative transmitted pressures that result from impact of a Nylon ball at about 55 ft/sec were measured [2] for various coating types. These are of interest and can be compared with the crushing strength of the epoxy resin in the glass fabric laminate substrate. To make this comparison meaningful, however, the correspondence between the pressure developed by a waterdrop impact at 500 mi/hr (733 ft/sec) and that developed by a Nylon ball impinging at about 55 ft/sec needs to be determined. The time required for the rubbery coating to spring back or recover after the impact has occurred also needs to be measured in order to determine if recovery time is an important characteristic as far as rain-erosion resistance is concerned.

The work described in this report has been directed toward realizing four objectives related to the performance of protective radome coatings: to determine with greater confidence whether or not composite coatings provide better protection against erosion than conventional single-layer coatings (see Section 2), to work toward development of a method to measure the recovery time after impact of a rubbery coating bonded to a rigid substrate (see Section 3), to establish the correspondence between the pressure generated by a Nylon ball impact at about 55 ft/sec and a waterdrop impact at 500 mi/hr for at least one material (see Section 4), to explore new waterdrop impact test methods (see Section 5).

2.

## 2. RAIN-EROSION, SAND-AND-DUST EROSION, AND WEATHERING RESISTANCE OF SELECTED COMPOSITE AND SINGLE-LAYER COATINGS

In a single set of rotating-arm test results obtained with use of flat specimens [2], a composite coating (HS) consisting of a soft polyurethane overcoated with a hard polyurethane and a single-layer coating (S) consisting wholly of a soft polyurethane both outperformed a single-layer coating (H) consisting wholly of a hard polyurethane. The relative rating found for the coatings (HS) and (S) is not significant because of the scatter in the test results; it needs to be verified by further testing. Results of tests for resistance to sand-and-dust erosion and for resistance to high speed waterdrop impacts both before and after weathering are given in this section for these coating types.

Studies carried out [1] with a computer program that sums the effect of arrival of elastic plane waves at the substrate surface after multiple reflections and transmissions in a coating show that introduction of a thin layer of very hard material (stress bumper) between the hard topcoat and soft undercoat of a composite coating reduces the initial rate of loading at the substrate that follows an impact against the surface of the coating. The stress bumper layer increases reflection and reduces transmission of incoming stress waves. Reduction of the initial rate of loading should have the effect of protecting not only a fragile glass fabric laminate substrate but also of protecting the adhesive bond between coating and substrate. Consequently, a composite coating that contains a stress bumper should outperform a simple two-layer composite coating. Rain-erosion test results for a stress bumper composite coating are given in this section.

Studies with the computer program also indicated that introduction of several transition layers of progressively decreasing hardness between the hard topcoat and soft undercoat of a two-layer composite coating (graded coating) should have merit. Not only is there a possibility of lower loading rate for the multi-layer coating in comparison with the two-layer coating but, in

3.

addition, the shear stresses that develop between coating layers should be less in the case of graded coatings than in the case of two-layer coatings. This follows because the properties of the successive layers of a graded coating are not widely different. It has, indeed, been recognized that, from the standpoint of adhesion, the most desirable interface between a coating and a bulk material is one in which the composition of the interface is graded from that of the coating material to that of the bulk material [4].

The feasibility of applying multilayer polyurethane coatings to radomes has been questioned. The objection has been that a coating procedure which requires, say, five different coating materials that must be applied in a given order is too detailed to be practical. Actually, five different coating materials are not required. The coating materials required are the same as in the case of a two-layer composite coating, namely, a softcoat (S) and a hardcoat (H). It is only the way in which they are applied that is different. To form the two-layer coating, a softcoat is sprayed to an arbitrary depth; this requires several passes with the spray gun. Then the hardcoat is sprayed over the soft under-coat; this also requires several passes with the spray gun. To form a graded multilayer coating, one pass with the spray gun is made using the softcoat material. With each succeeding pass, hardcoat material is added to the spray gun reservoir until the final pass is made with pure hardcoat material.

Regardless of application feasibility considerations, the graded multilayer coating concept has interesting possibilities. If it is ruled out as impractical for an entire radome, it can, nevertheless, be used in the production of coating boots. Rain-erosion test results for a graded multilayer coating are given in this section.

## 2.1 PREPARATION OF COATING SPECIMENS

Two basic moisture-cured polyurethane coating materials were used to make the four coating types. These were coating materials $S_2$ with a Shore A hardness of 55-56 and $H_1$ with a Shore A hardness of 75-76. These polyurethane materials were prepared and the coating application work was done under the supervision of Mr. J.F.Moraveck at Olin Research Center, New Haven, Conn.

In view of the finding that the curvature of airfoil shaped test specimens causes coatings to fail in fatigue as a consequence of unequal yield under high speed waterdrop impingement [2], all of the coating types were applied to flat substrates. For use on the Bell Aerospace Company rotating-arm tester, the flat specimens were 0.375 (+.000, -.031) inch wide and 1.5 inch long with reasonable tolerance. For use on the British Royal Aircraft Establishment rotating-arm tester, the flat specimens were square with an edge length of one inch with reasonable tolerance.

The substrate material used for the rotating-arm test specimens was nominal 1/8-inch-thick, research quality, glass fabric laminate sheet that was prepared by Brunswick Corporation, Marion, Va. The glass fabric laminate sheet was prepared with use of Cordopreg E-293 to meet Mil R 9300 specifications. For laboratory tests of the pressure felt at the substrate beneath a coating, loading rate at the substrate, and impact energy accepted by the coating, the four coating types were also applied to 20-mil-thick Alclad 2024 aluminum Q-panels. Aluminum rather than glass fabric laminate was chosen as the substrate material for the laboratory tests because a much lower percent deviation between individual determinations and, consequently, better resolution of the relative performance of coating types in these tests, was found [2] using aluminum substrates.

The total thickness of each of the coatings was held to 15 mils as far as this could reasonably be controlled. The single-layer soft polyurethane coating consisted of a 15-mil thickness of

the $S_2$ polyurethane. To form the two-layer composite coating, a 6-mil layer of $S_2$ was applied to the substrate; this layer was overcoated with 9 mils of $H_1$ polyurethane. To form the stress-bumper coating, a 5-mil layer of $S_2$ was applied to the substrate; this layer was overcoated with a 5-mil layer of $H_1$; a 5-mil layer of $S_2$ was then applied as the surface topcoat. It is noteworthy that this is a different stress-bumper coating from the one studied with use of the computer program; the change was made to avoid problems in making a hard polyurethane or in use of other material for the stress-bumper layer and to take advantage of the low impact stress that is generated on a soft surface coating. To form the graded multilayer coating, a 3-mil layer of $S_2$ was applied to the substrate; this was overcoated successively with 3 mils of a blend of 75 parts of $S_2$ with 25 parts of $H_1$, 3 mils of a blend of 50 parts of $S_2$ with 50 parts of $H_1$, and 3 mils of a blend of 25 parts of $S_2$ with 75 parts of $H_1$; the topcoat was 3 mils of $H_1$.

The specimens were prepared by spraying a large flat panel of the glass fabric laminate with the specific coating and then sawing specimens of the required size and tolerance from this panel. The glass fabric laminate sheet to be used as substrate material came with a rough textured surface. It was used in the as-received condition without any additional abrasive roughening; the surface of the glass fabric laminate substrate was solvent rinsed before spraying on the primer and then the coating.

In the case of the oblong test specimens used on the Bell Aerospace Company rotor the specimens were sawed from a coated piece of laminate in such a way that the woof fibers ran perpendicular to the direction of the specimen length. In weaving cloth, the warp threads run lengthwise in the loom; the woof or weft threads are woven across the fixed warp threads in such a way that they pass alternately above and below the successive warp threads. This causes the woof threads to protrude above the level of the warp threads on both sides of the cloth. If this texture is not obliterated (by being filled with resin) when glass cloth is fabricated into a laminate to which a radome coating is applied, the protruding woof fibers will serve as

restraints to the slippage of the coating under centrifugal force during a rotating-arm test. Maximum restraint is imposed if the warp fibers of the topmost layer of cloth run in the direction in which centrifugal force acts; the direction in which protruding woof fibers run will then be perpendicular to the direction in which centrifugal force acts.

The square shape of the specimens used on the British Royal Aircraft Establishment rotor left the selection of the direction in which the protruding woof fibers run to the person who would mount the specimen on the rotor. In the case of these square specimens, an arrow running perpendicular to the woof fibers was drawn on the rear face of the specimen. The specimens were mounted on the rotor in such a way that the arrow pointed in the direction in which centrifugal force would act during the test.

The total thickness of each coating type that was prepared was measured. Thickness measurements made on the aluminum panels were considered to be the most accurate. The measured thicknesses of the four coating types as determined in this way were reported by Mr. Moraveck to be as follows: two-layer composite coating, 14.4 mils; single-layer coating, 14.2 mils; graded multilayer coating, 14.9 mils; stress-bumper coating, 14.4 mils.

Before the specimens were sent for test, they were inspected at low magnification with use of a Bausch and Lomb stereomicroscope. It was observed that adhesion-loss runners between coating and substrate were generated along the edges of the specimens by the sawing operation. The stress-bumper coating appeared to be somewhat more susceptible to this. For the cases for which runner length was measured, it was found to be less than 50 mils. It was hoped that these runners would be covered by the restraining frame that holds a specimen to the rotor. This was probably the case except for those specimens that moved under the restraining frame under the action of centrifugal force.

In roughly half of the specimens of each of the four coating types, a few stray adhesion-loss runners were observed on the test area of the coating specimen itself as well as at the saw cut. These specimens were considered to be questionable and they were separated from the specimens to be tested. Regrettably, there were not enough perfect specimens of the two-layer composite coating, $H_1S_2$, for the tests to be run on the Bell Aerospace Company rotor. It was necessary to select the four best of the rejected specimens of this coating type and submit them for test. The four selected specimens had runner defects close to the edge. Photomicrographs were made of the defects and a record was kept of their locations on the specimens to make it possible to determine, after the tests were run, whether or not these defects affected the test lifetimes of the specimens.

Three square specimens of each of the coating types were sent for test of high speed rain-erosion resistance under the direction of Mr. Andrew A Fyall at the British Royal Aircraft Establishment, Farnborough, Hants, England. Four rectangular specimens of the stress-bumper coating and of the graded multi-layer coating and eight rectangular specimens of the two-layer composite coating and of the single-layer coating were sent for test under the direction of Mr. Norman E. Wahl at Bell Aerospace Company, Buffalo, N.Y. Four of the two-layer composite coating specimens and four of the single-layer coating specimens sent to Bell Aerospace Company were for test of high speed rain-erosion resistance; the other four specimens of these coating types were for test of sand-and-dust erosion resistance. Four rectangular specimens of both the two-layer composite coating and the single-layer coating were retained for weathering prior to test for rain-erosion resistance on the rotating-arm device at Bell Aerospace Company.

## 2.2 RESULTS OF ROTATING-ARM TESTS AT BELL AEROSPACE COMPANY

The test specimens received at Bell Aerospace Company were stored in a dessicator at 50 percent relative humidity until the tests could be run; the waiting period was about one month. The specimens were tested at an impact velocity of 500 mi/hr (733 ft/sec) in a 1-inch/hour simulated rain of 1.8- to 2.0-mm drops. The test chamber was evacuated to a pressure of 250 mm mercury to minimize as far as feasible deflection of drops as a consequence of buildup of air cushions on the specimens during test.

### 2.2.1 Specimens Tested for Rain-Erosion Resistance Prior to Weathering

Four specimens of each of the four coating types were tested for rain-erosion resistance at the end of the one-month waiting period during which they were stored under optimum conditions. When the tested specimens and the data on their test lifetimes were received, the specimens were examined at low power with use of a Bausch and Lomb stereomicroscope. This revealed that six of the sixteen specimens tested had not yet developed a hole through the coating. Because the arbitrary criterion of failure that has been used in this study is formation of a hole through the coating, these specimens were returned to the testing laboratory for continuation of their tests.

During the microscopic inspection of the specimens three modes of failure were monitored; these were hole formation, crack formation, and adhesion loss. The test lifetimes and the extent to which the three modes of failure that were monitored had progressed are given in Table 1 for the condition that the failure criterion of hole through the coating was not reached for six of the specimens. A picture of the specimens of the four coating types that was taken after each of the specimens was ter ed to the point of formation of a hole through the coating is shown in Figure 1.

TABLE 1

RESULTS OF INSPECTION OF COATING SPECIMENS TESTED AT BELL AEROSPACE COMPANY WITH RAIN

SINGLE-LAYER COATING $S_2$

| Spec'm No & Test Time / Type of Failure | No. 1 20 min | No. 2 30 min | No. 3 25 min | No. 4 40 min |
|---|---|---|---|---|
| HOLES | 1 small with cracks at end of specimen | 1 large with crack at end of specimen | 1 small at center of specimen | 1 large with cracks at end of specimen |
| CRACKS | 1 isolated at end of specimen | 2 isolated at end of specimen | 2 large isolated at one end of spec'm 2 small isolated at opposite end | No isolated cracks |
| ADHESION LOSS | No evidence of adhesion loss except around a hole | No evidence of adhesion loss except in vicinity of crack and large hole | Small adhesion-loss runners at one end; adhesion loss in vicinity of a crack and hole | Slight evidence of adhesion-loss runner formation. Adhesion loss around hole. |

TWO-LAYER COMPOSITE COATING $H_1S_2$

| Spec'm No & Test Time / Type of Failure | No. 1 45 min | No. 2 45 min | No. 3 45 min | No. 4 18 min |
|---|---|---|---|---|
| HOLES | 1 with radial and peripheral cracks | 1 with cracks near center of specimen | No holes | No holes |
| CRACKS | 2 large isolated | 2 medium isolated | 2 isolated star shaped | 1 that was probably under frame |
| ADHESION LOSS | Small amount associated with protruding woof fibers; also near cracks and hole | Small amount on protruding woof fibers; some runners along glass fibers; adhesion loss near hole & crk. | Small amount on protruding woof fibers | Heavy adhesion loss along glass fibers at one end of specimen. |

10.

TABLE 1, CONTINUED

MULTILAYER COMPOSITE COATING $H_1H_2H_3S_3S_2$

| Spec'm No. & Test Time / Type of Failure | No. 1  30 min | No. 2  40 min | No. 3  40 min | No. 4  40 min |
|---|---|---|---|---|
| HOLES | 9 holes counted | No holes | No holes | No holes |
| CRACKS | about 35 counted | 1 in center area | 1 near center and 1 small near end of specimen | 2 large cracks |
| ADHESION LOSS | Adhesion loss associated with cracks and holes | Adhesion loss on protruding glass woof fibers at one end (?) | Adhesion-loss runners along glass fibers at one end | Adhesion loss along glass fibers at one end |

STRESS-BUMPER THREE-LAYER COMPOSITE COATING $S_2H_1S_2$

| Spec'm No. & Test Time / Type of Failure | No. 1  40 min | No. 2  29 min | No. 3  8 min | No. 4  28 min |
|---|---|---|---|---|
| HOLES | 1 with cracks & adhesion-loss bubble at end of specimen | 1 just opened from crack at end of specimen | No holes | 1 with radial cracks at specimen center |
| CRACKS | No isolated cracks | 6 small at one end of specimen 2 large at opposite end of specimen | 1 at one end and 1 small at opposite end of specimen | 1 very small at edge in center of specimen |
| ADHESION LOSS | Adhesion-loss runners along glass fibers all over specimen; adhesion loss at hole | Adhesion-loss runners along glass fibers all over specimen; heavy at one end | Adhesion loss along glass fibers at one end | Adhesion-loss runners along glass fibers relatively small in amount; adhesion loss at hole |

11.

SINGLE-LAYER COATING $S_2$

TWO-LAYER COMPOSITE COATING $H_1S_2$

MULTILAYER COMPOSITE COATING $H_1H_2H_3S_3S_2$

STRESS-BUMPER COMPOSITE COATING $S_2H_1S_2$

FIGURE 1. FOUR TYPES OF POLYURETHANE COATING AFTER RAIN-
EROSION TEST AT BELL AEROSPACE COMPANY.
Left to right are Specimens 1 to 4.

## Single-Layer Coating of Soft Polyurethane $S_2$

Each of the four specimens of the single-layer softcoat, $S_2$, was tested to the point of failure as indicated by formation of a hole through the coating (see Table 1). For two of the specimens the hole that formed is large; for the other two it is small.

Cracks that are completely isolated from other damage formed on three of the specimens. The isolated cracks on Specimen No. 1 and Specimen No. 2 are accompanied by removal of material at the surface of the coating. Judging from the position of its shadow, as observed with use of the microscope, the isolated crack on Specimen No. 1 does not extend completely to the substrate; this suggests that it may have originated at the surface or at a defect within the coating. Both isolated cracks on Specimen No. 2 extend completely through the coating; there are adhesion-loss runners at the substrate level under the larger of these two cracks.

Both large cracks at the high-speed end of Specimen No. 3 extend from the coating surface to the substrate. The smaller of the two is accompanied by material loss at the surface of the coating; the larger crack is accompanied by adhesion-loss runners at the substrate level. The two small cracks at the low-speed end of Specimen No. 3 are located at the surface of the coating; neither is accompanied by loss of coating material. Judging from the position of their shadows, as observed with use of the microscope, they have not reached the substrate or have reached it only at one point.

Because the specimens were flat, the irrelevant stress of unequal yield [2] was eliminated. However, there is some evidence that the restraining frame that holds the flat specimens to the rotor may provide a machine effect that could play a role in the failure of specimens. Specimen No. 4 may have a frame induced crack near the hole through the coating (see upper right picture of Figure 2). This crack runs parallel to the edge of the specimen at a distance from the edge that corresponds roughly with the width of the restraining frame. There is, however, no evidence

Single-Layer $S_2$, Spec. No. 4
Adhesion Condition at Specimen
Center after 40 minutes Test, 15X

Single-Layer $S_2$, Spec. No. 4
Hole and Evidence of Incipi-
ent Frame Crack, 7.5X
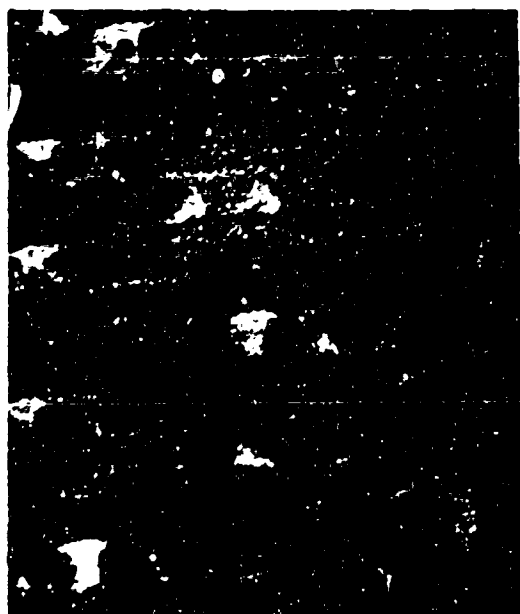
Two-Layer $H_1S_2$, Spec. No. 1
Adhesion Condition at Specimen
Center after 45 Minutes Test, 15X
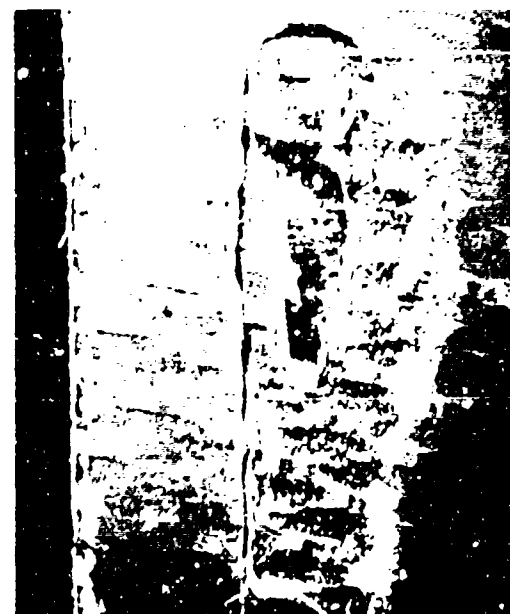
Two-Layer $H_1S_2$, Spec. No. 4
Hole and Crack Along Frame
after 44 Minutes Test, 7.5X

FIGURE 2.    MAGNIFIED VIEWS OF DAMAGE ON SINGLE-LAYER COATING
            AND TWO-LAYER COMPOSITE COATING

14.

that this particular crack was involved in the formation of the hole through the coating.

The observations that were made with regard to cracks suggest that isolated fatigue cracks may form at the surface of a coating and grow toward the substrate. Material can be broken out of the coating surface along a growing crack as a consequence of additional drop impacts and/or of the high-speed flow of accumulated drop liquid which is driven by centrifugal force over the surface of the coating. When a crack is sufficiently deep, material loss may be extensive enough to result in hole formation.

For Specimens No. 1 and No. 2 there was no evidence of adhesion loss except at the sites of cracks and holes but the test lifetimes of these specimens were only 20 and 30 minutes, respectively. In the case of Specimen No. 3, which failed after 25 minutes of test, small adhesion-loss runners formed between glass fibers at one end of the specimen and in the case of Specimen No. 4, which had a test lifetime of 40 minutes, there was evidence of incipient adhesion-loss runner formation.

The specimens of single-layer $S_2$ coating tested in 1974 differ from specimens of single-layer $S_2$ coating tested in 1973 in that no evidence of isolated cracks or of adhesion-loss runners was reported [2] in 1973. Adhesion loss that developed on $S_2$ single-layer coatings in 1973 was associated with protruding woof fibers and resembled the adhesion loss that developed on the $H_1 S_2$ two-layer coating in 1974 (see lower left picture of Figure 2).

The test lifetimes in minutes obtained for specimens of single-layer $S_2$ coating in 1973 and 1974 are tabulated below.

| Year | Test Lifetimes of Specimens, minutes | | | | Average Lifetime, min |
|------|------|------|------|------|------|
| 1973 | 45 | 51 | 50 | -- | 48.7 |
| 1974 | 20 | 30 | 25 | 40 | 28.9 |

15.

To determine by a statistical method if there is a significant difference in the average lifetime values, the assumption that the average values are equal was tested by calculating the value of t. The one percent critical value of t was found to be 3.365. The calculated value of t was found to be 3.9. Because the calculated value of t exceeds the critical value, the average test lifetimes for the single-layer $S_2$ coating found in 1973 and 1974 are significantly different.

Based on the evidence of the test lifetimes, the evidence of formation of isolated cracks in 1974, and the evidence of formation of adhesion-loss runners in 1974, the single-layer $S_2$ coating prepared and tested in 1973 either had better rain-resistance than that which was prepared and tested in 1974 or the testing conditions were more severe in 1974.

## Two-Layer Composite Coating $H_1S_2$

Two of the four defective specimens of the two-layer composite coating (see Section 2.1) were used in the rotating-arm tests. They were tested as Specimen No. 2 and Specimen No. 4. These specimens contained adhesion-loss runner defects that were relatively close to the specimen edge. The defects were located with use of the microscope after the specimens were tested. They were found to be just as they appeared prior to test. On this basis it was concluded that they in no way affected the failure or the test lifetime of these specimens.

Specimen No. 3 and Specimen No. 4 contained no holes after 45 and 18 minutes of test, respectively (see Table 1). Their tests were continued. Specimen No. 3 picked up 18 minutes of additional test time before a hole formed. The coating lifted at the high-speed end of the hole and a deposit of white debris accumulated under the coating blister (see Figure 1). Specimen No. 4 picked up 26 additional minutes of test time before two holes formed through the coating. Both holes formed at the edge of the restraining frame that holds a specimen to the rotor (see Figure 1 and lower right picture of Figure 2); the other hole

formed in the area of heavy adhesion loss (see Table 1 and Figure 1).

One of the two large cracks on Specimen No. 1 is star shaped. Both cracks on this specimen extend from the surface of the coating to the substrate. The two medium small cracks on Specimen No. 2 also extend from the surface of the coating to the substrate. Two star-shaped cracks were observed on Specimen No. 3 at the end of 45 minutes of test. These cracks appear to have been involved in formation of the hole through the coating during the additional period of test that this specimen was given because, at the end of the additional period of test, there were no isolated cracks on this specimen. This is evidence that at least some hole formation is a consequence of the growth of cracks in a coating. There is only one isolated crack on Specimen No. 4. This crack, which opened during the additional period of test given to this specimen, is in the area of heavy adhesion loss at the high-speed end of the specimen.

The adhesion loss sustained by the specimens of the two-layer composite coating $H_1S_2$ resembles the adhesion loss that occurred on $H_1S_2$ coating specimens in 1973. It starts at protruding coof fibers (see lower left picture of Figure 2) and progresses along the glass fibers [2] with lapse of time. Specimen No. 4 differed from the other three specimens of the two-layer composite coating in that it developed heavy adhesion loss along glass fibers at the high-speed end after only 18 minutes of test.

The appearance of Specimen No. 3 and Specimen No. 4 after their tests were continued to the point of hole formation was informative. In the case of Specimen No. 3, cracks and adhesion-loss runners formed along the position of the restraining frame. In the case of Specimen No. 4, cracks and adhesion-loss runners formed along the position of the restraining frame and cracks formed in areas of adhesion loss (see lower right view of Figure . This is evidence that the restraining frame used to hold flat specimens to the rotor does play a role in the failure of the specimens. Failure brought on by a machine effect is irrelevant as far as the true rain-erosion resistance of a coating is concerned but it can be informative. A possible cause of crack

formation along the restraining frame is that the restraining
frame itself provides a line along which there is unequal yield
within the coating.  Unequal yield has been identified with for-
mation of fatigue cracks [2].

The test lifetimes of the specimens of two-layer composite
coating $H_1S_2$ that were tested in 1973 and 1974 are given below:

| Year | Test Lifetimes of the Specimens, minutes | | | | Average Lifetime, min |
|------|------|------|------|------|------|
| 1973 | 55 | 70 | 44 | 36 | 51.2 |
| 1974 | 45 | 45 | 63 | 44 | 49.2 |

The value of average lifetime obtained in 1974 compares favorably
with the value of average lifetime obtained in 1973.  The similar-
ity in the average lifetime for these two sets of $H_1S_2$ coating
is evidence that the severity of the testing conditions was sim-
ilar in 1973 and 1974.  In retrospect, the poor performance of the
$S_2$ single-layer coating in 1974 in comparison with the perform-
ance of the same coating in 1973 suggests that the $S_2$ single-
layer coating prepared and tested in 1973 was of better quality
as far as rain-erosion resistance is concerned.

Multilayer Composite Coating   $H_1H_2H_3S_3S_2$

Specimen No. 1 of the multilayer composite coating exhib-
ited quite unusual behavior in that cracks formed all over its
surface.  A section of the all-over crack pattern is shown in the
upper left picture of Figure 3.  The cracks ranged in complexity
from simple isolated straight and curved cracks to cracks with
many branches.  There are two large holes (see Figure 1) on this
specimen and seven additional small holes associated with the
cracks.  There is one instance in which a hole has formed on a
single isolated straight crack.  It is possible that a branch
crack that may have existed could have been eliminated at the
time the hole formed. There is no evidence on this specimen of a

Multilayer Coating Spec. No. 1
All-Over Pattern of Cracks 7.5X

Multilayer Coating Spec. No. 3
Crack that Accumulated Adhesion Loss and Formed Hole 7.5X
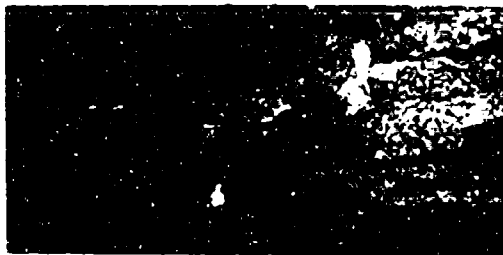
Stress-Bumper Spec. No. 1 & 2
Adhesion Loss Accumulating
Along Glass Fibers   15X

Stress-Bumper Specimen Prior
to Test Showing Adhesion-Loss
Runners along Saw Cut 22.5X

FIGURE 3.   MAGNIFIED VIEWS OF DAMAGE ON MULTILAYER COATING
AND STRESS-BUMPER COATING

crack associated with the restraining frame.  This specimen was so very different from the other three specimens of multilayer coating in its response to drop-impingement test that it could be regarded as a questionable specimen.

Specimen No. 2 of the multilayer coating had no holes after 40 minutes of  test.  After 14 minutes of additional test, cracks associated ith the restraining frame formed along both sides of this specimen.  Branch cracks ran out into  the coating from the frame cracks and the coating  broke away along the frame crack on one side of the specimen.  The one crack that existed after 40 minutes of test developed and widened at one point to form  a hole during the period of  additional test.

Specimen No. 3 of the multilayer coating had no holes after 40 minutes of test.  After 20 minutes of additional test there was evidence of cracks associated with the restraining frame along both sides and both ends of this specimen.  A crack observed at the center of  the specimen after 40 minutes of  test enlarged as a result of continued test.  It developed a circular area of adhesion loss and opened at one end to form a hole (see upper right picture of Figure 3).  A small crack observed near one  end of the specimen after 40 minutes of test presumably grew into the large crack that exists there after 60 minutes  of test.  In addition, a large branched crack formed at the opposite  end of the specimen.  Both of these cracks have widened enough to expose the primer at the substrate level.  Loss of adhesion, which at the end of 40 minutes of  test was restricted to adhesion-loss runners along glass fibers at what appeared to be the high-speed end of the specimen, worsened during the period of additional test.

Specimen No. 4 of the multilayer coating had no holes after 40 minutes of  test.  After 20 minutes of additional test, a crack associated with the restraining frame formed along the sides and especially along  one of the ends  of this specimen.  Loss of adhesion, which was restricted to adhesion loss along glass fibers at the  specimen  end after 40 minutes of test, worsened as  a result of continued test; cracks opened in  the area of adhesion

loss and coating material broke away.  There are two isolated cracks on this specimen after 60 minutes of test; one of these is at the center and the other is at one of the ends of the speci-men.

The test lifetimes in minutes of specimens of the multi-layer coating, after all specimens were tested to the point of hole formation, are as follows:

| Test Lifetimes of the Specimens, minutes | | | | Average |
|---|---|---|---|---|
| No. 1 | No. 2 | No. 3 | No. 4 | Lifetime, min |
| 30 | 54 | 60 | 60 | 51.0 |

If the 30-minute lifetime of Specimen No. 1 were to be discarded as questionable, the average lifetime of the multilayer coating would be 58.0 minutes.  Inquiry was made to determine if there was any circumstance that was different about the test conditions for this specimen but no difference came to light.  On this basis it seems preferable to retain the test lifetime of Specimen No. 1 in evaluating the performance of the multilayer coating because there were instances of some degree of unusual behavior among the specimens of the other coating types as well.

The average test lifetime of 51.0 minutes for the multilayer coating is about the same as the 49.2-minute average lifetime of the two-layer composite coating.  If one compares the overall state of damage of  the specimens of these two types of composite coating (see Figure 1), it appears that the specimens of  the two-layer composite coating are less damaged at the end of their average lifetime than the specimens of  the multilayer coating.

## Stress-Bumper Composite Coating    $S_2H_1S_2$

The stress-bumper coating was designed to provide maximum reflection of the impact pressure pulse to reduce the rate of loading at the substrate level and in this way protect the

fragile primer and glass fabric laminate substrate from failure that might lead to a loss of adhesion of the coating. Surprisingly, while the formation of holes and cracks in the stress-bumper coating specimens was comparable to that observed in specimens of the other coating types (see Table 1), the distinctive feature of the tested specimens of stress-bumper coating was marked evidence of adhesion loss. This behavior is interesting in that it may provide a new clue to understanding the mechanism of adhesion loss in radome coatings in general. This is discussed further below.

Specimen No. 1 had a test lifetime of 40 minutes which compares favorably with long test lifetimes of the other three coating types (see Table 1). This specimen contained no isolated cracks; the presumption is that an isolated crack that it did contain was obliterated in the formation of the hole through the coating. Two of the other three specimens of stress-bumper coating contained isolated cracks as well as holes. Specimen No. 3 had no holes at the end of eight minutes of test. When test of this specimen was continued, it picked up 32 additional minutes of test time giving it a test lifetime of 40 minutes before it failed.

The test lifetimes of the four specimens of stress-bumper coating are as follows:

| Test Lifetimes of the Specimens, minutes | | | | Average |
|---|---|---|---|---|
| No. 1 | No. 2 | No. 3 | No. 4 | Lifetime, min |
| 40 | 29 | 40 | 28 | 34.2 |

The presence of the layer of hardcoat. $H_1$, introduced into the middle of t! stress-bumper coating appears to have given it a somewhat longer average test lifetime than the single-layer $S_2$ coating. Application of a statistical test of significance, however, indicated that the difference between the average lifetime of these coating types is not significant.

Specimens of single-layer $S_2$ coating showed very little evidence of adhesion loss and this is in agreement with earlier observations [2]. It has been thought [2] that a polyurethane softcoat forms a stronger bond to the substrate than a polyurethane hardcoat and that this explains its greater resistance to adhesion loss. Contrariwise, the stress-bumper coating has $S_2$ softcoat in contact with the substrate; it also has $S_2$ softcoat at the impact surface so that the magnitude of the impact pressure pulse is the same as that generated on a single-layer $S_2$ softcoat. The stress-bumper coating differs from the single-layer $S_2$ coating only in that a layer of hardcoat, $H_1$, has been introduced into the middle of it. The layer of hardcoat within the stress-bumper coating causes extensive reflection of the impact pressure pulse within the coating. This can be expected to result in vibration of the coating. Vibration of the coating, in turn, may break the adhesive bond between the coating and substrate.

This observation may correlate with and may afford a new explanation of the experimental finding noted above that a hard polyurethane coating loses adhesion to the substrate whereas a soft polyurethane coating does not. Resilience measurements [2] showed that a hard polyurethane coating absorbs or dissipates a much smaller amount of impact energy than a soft polyurethane coating. This is an index to the damping characteristics of these coatings; the softcoat damps out the pressure pulse but in the hardcoat the pressure pulse may reverberate for a long time before it is damped out. The reverberation of the pressure pulse in the hardcoat results in vibration which, in turn, may break the adhesive bond that holds the coating to the substrate. Poor damping characteristics could conceivably be the cause of the known failure of hard coatings and paints that have been tested for rain-erosion resistance.

The observed loss of adhesion of the stress-bumper coating during rain-erosion test (see lower left pictures of Figure 3) correlates with the copious formation of adhesion-loss runners along the edges of the specimens when the specimens were sawed to size and shape (see Section 2.1). Sawing is a vibration

23.

producing operation. This suggests that sawing a cut into a
coating that is applied to a substrate and noting the amount of
adhesion loss generated at the edge of the saw cut may provide
a useful indication of adhesion characteristics. It would be
necessary to study the amount of adhesion loss generated in this
way in coatings that have widely different adhesion character-
istics and to determine the effect of variables such as the rate
of sawing and the size of the piece of coated substrate used.

### 2.2.2 Specimens Tested for Rain-Erosion Resistance
### After Weathering

The single-layer coating $S_2$ and the two-layer composite
coating $H_1S_2$ were tested for rain-erosion resistance after
weathering. The first stage of weathering was outdoor exposure
in a sunny location. The purpose of this stage of weathering
was to determine the response (possible rupture of bonds) to
ultraviolet light, humidity, and ozone. A weathering rack to
hold four specimens of each of these two coating types securely
and yet loosely enough to allow for expansion in the heat of
the sun was designed and constructed. This rack was attached
to the roof structure of the Mechanical Engineering Building at
Florida Atlantic University, Boca Raton, Fla. The specimens
were put out on the rack on March 11. Because a considerable
length of time was required to have the test specimens prepared,
the first stage of weathering had to be restricted to ten weeks.

The specimens were removed from the rack on May 17. They
were observed to have darkened uniformly in color and to have a
surface accumulation of dust and sand grains. They were washed
with running water and rubbed lightly to dislodge the dust and
sand grains. They were then air dried and divided into two
groups consisting of two specimens of each of the two coating
types. One of these groups of specimens was stored under opti-
mum conditions of temperature and humidity. The other group
was subjected to a second stage of weathering.

The second stage of weathering was designed to test the
response (possible loss of solvent) to reduced air pressure at

24.

high altitudes. Two specimens of each of the two coating types
that had weathered outdoors for ten weeks were put into a vacu-
um dessicator. With use of a mercury manometer and the Chemis-
try Department vacuum line, the pressure in the dessicator was
brought to 3.44 inches (87.4 mm) mercury; this is the air pres-
sure at an altitude of 50,000 feet. The specimens were main-
tained at this reduced pressure for 12 days; they were removed
from the dessicator on May 29. During this time interval, the
pressure in the vacuum dessicator was checked twice to insure
that it remained constant. No change of the pressure was ob-
served.

At the end of the second stage of weathering, all of the
weathered specimens were inspected with use of a stereomicro-
scope. This inspection failed to show changes that were clearly
related to the weathering processes. Some residual sand grains
were observed; these appeared to be embedded in the surface lay-
ers of the coatings. Some flat structures not observed before
were noted. In particular, it was noticed for the first time
that protruding woof fibers were bare of primer in one part or
another of the specimens. Primer denudation of protruding woof
fibers, which was thought earlier [2] to be an effect of rain-
erosion test, is presumably a result of neglecting to change the
position of a glass fabric laminate sheet or specimen during the
initial stage of drying after it is sprayed with primer. The
relative importance of this condition is not known but it has
been observed [2] that incipient adhesion loss starts on protrud-
ing woof fibers and, consequently, to the extent that primer den-
udation of protruding woof fibers exists, the specimens are not
strictly comparable. As an aid in the analysis of damage incurred
by tested specimens, the testing laboratory was requested to mark
the end of the specimen that occupied the high-speed position
in each test run.

The weathered specimens of $S_2$ single-layer coating and $H_1S_2$ composite coating were tested for rain-erosion resistance on the Bell Aerospace Company rotor with use of the same conditions that had been used for the specimens that were tested prior to weathering. Two of the $H_1S_2$ specimens had been rejected because of the presence of defects but had been subjected to weathering and sent for test because there were not enough defect-free specimens among the specimens of $H_1S_2$ coating that had been prepared. One of the questionable specimens was tested as Specimen No. 1 of the $H_1S_2$ specimens that were exposed to weather alone. The other had either not been labeled or had lost its identifying label. The defect on $H_1S_2$ Specimen No. 1 should have been covered by the restraining frame; it was not located on the tested specimen.

The tested specimens are shown as a group in Figure 4A. Visual inspection of the tested specimens indicated that they had slipped under the restraining frame and moved toward the high speed end of the rotor (as indicated on the reverse side of the specimens) to the extent that the frame barely covered the opposite end of the specimen. Comparison of the extent of frame coverage with the test lifetimes indicated that the extent of frame coverage probably did not affect the test lifetimes. By visual inspection it could also be seen that the high gloss characteristic of polyurethane coatings was removed to different degrees from the tested weathered specimens.

The reported test lifetimes of the two coating types for the case that they were exposed to weather alone and for the case that they were exposed to weather and then to the reduced pressure corresponding to an altitude of 50,000 feet are given in Table 2A. From the average lifetime values found for the weathered specimens, it can be seen that exposure to the weather for ten weeks resulted in a strong reduction in rain-erosion resistance. The lifetimes of the single-layer softcoat and of the two-layer composite coating were reduced to 18 percent and to 6 percent of their lifetimes before weathering, respectively. On the basis of the test results obtained, the presence of a hard transparent topcoat does not protect a soft undercoat from weathering

26.
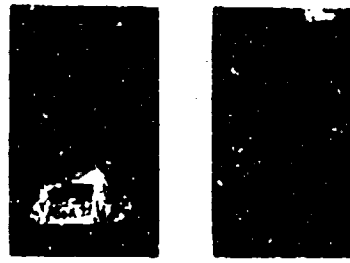
$S_2$ WEATHER ONLY $\qquad$ $S_2$ WEATHER AND LOW PRESSURE

$H_1S_2$ WEATHER ONLY $\qquad$ $H_1S_2$ WEATHER AND LOW PRESSURE

A. SPECIMENS OF $S_2$ AND $H_1S_2$ TESTED FOR RAIN-EROSION RESISTANCE AFTER WEATHERING WITH AND WITHOUT EXPOSURE TO LOW PRESSURE
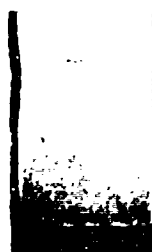
LEFT TO RIGHT ARE $S_2$ SPECIMENS 1 TO 4
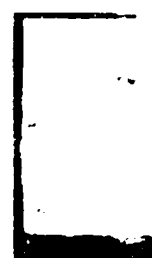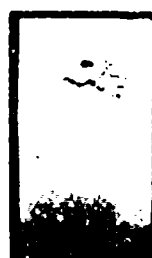
LEFT TO RIGHT ARE $H_1S_2$ SPECIMENS 1 TO 4

B. SPECIMENS OF $S_2$ AND $H_1S_2$ TESTED FOR SAND-EROSION RESISTANCE

FIGURE 4. TWO TYPES OF POLYURETHANE COATING TESTED FOR RAIN-EROSION RESISTANCE AFTER WEATHERING AND FOR SAND-EROSION RESISTANCE

27.

TABLE 2

## Test Lifetimes of Weathered Rain Eroded Specimens and of Sand Eroded Specimen

A. <u>Weathered Specimens Tested in Rain</u>

    1. Exposed to Weather Only (Specimen Designations WS and WHS)

| Test Lifetimes in Minutes | | | |
|---|---|---|---|
| Coating \ Specimen No. | 1 | 2 | Average |
| $S_2$ | 5.5 | 5.0 | 5.25 |
| $H_1S_2$ | 3.0 | 3.0 | 3.0 |

    2. Exposed to Weather and Low Pressure (Specimen Designations VS and VHS)

| Test Lifetimes in Minutes | | | |
|---|---|---|---|
| Coating \ Specimen No. | 1 | 2 | Average |
| $S_2$ | 7.0 | 4.8 | 5.9 |
| $H_1S_2$ | 4.0 | 4.5 | 4.25 |

B. <u>Sand Eroded Specimens</u>

| Test Lifetimes in Minutes | | | | | |
|---|---|---|---|---|---|
| Coating \ Specimen No. | 1 | 2 | 3 | 4 | Average |
| $S_2$ | 25.0 | 20.0 | 21.0 | 23.0 | 22.25 |
| $H_1S_2$ | 27.5 | 30.0 | 23.0 | 35.0 | 28.83 |

deterioration. Comparison of the lifetimes obtained after weathering alone with those obtained after both weathering and exposure to low air pressure shows that the low-pressure environment produced a small increase in test lifetime in all but one case rather than a further reduction.

The tested weathered specimens of the two coating types were examined at low magnification under the microscope. It was observed from inspection of the broken edges of the coatings that the coating material of every tested specimen had changed in color from colorless transparent to a bright amber yellow. This identifies the observed darkening of the coating specimens with the coating material itself rather than with the primer. It indicates that a change occurred within the polymeric material.

Microscopic inspection of the weathered specimens of $S_2$ coating showed that the originally glossy surface had become almost uniformly frosted ; a view on the surface of Specimen No. 1 is shown in the upper left picture of Figure 5. Coating material was broken away around the edge of the restraining frame (see Figure 4A). Adhesion-loss spots could be seen through the frosted surface but no cracks were observed and there were only one or two chips or holes in the central area of the specimens. Specimens of $S_2$ single-layer coating which were exposed to reduced air pressure after weathering differed only in that cracks were observed and chips were eroded from the coatings all over the surface of the specimens; the latter condition can be seen in the upper right view of Figure 5.

In the case of the weathered specimens of $H_1S_2$ two-layer composite coating, the originally glossy surface was also frosted but the frosting was discontinuous. A view on the surface of Specimen No. 1 is shown in the lower left picture of Figure 5. Cracks were observed in the coatings but the breakout of coating material was restricted to the vicinity of the restraining frame. Similar observations were made on the weathered specimens of $H_1S_2$ coating that were exposed to reduced air pressure; a view on the surface of Specimen No. 1 is shown in the lower right picture of Figure 5.

$S_2$   Spec. No. WS-1   15X
Continuous Frosting
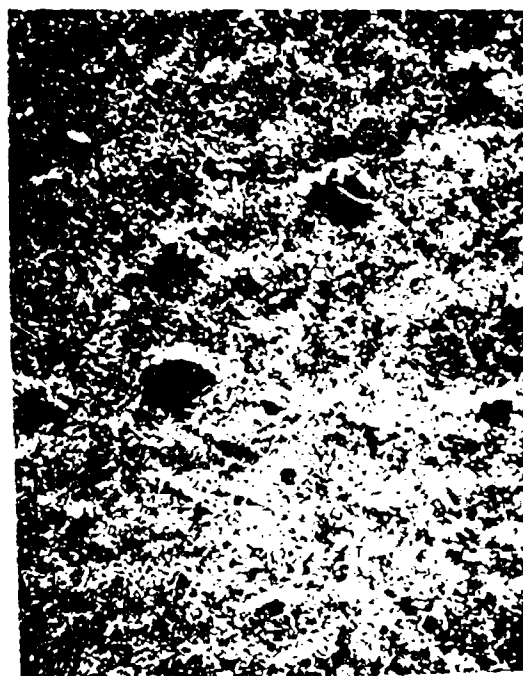
$S_2$   Spec. No. VS-1   15X
Continuous Frosting

$H_1S_2$   Spec. No. WHS-1   15X
Discontinuous Frosting
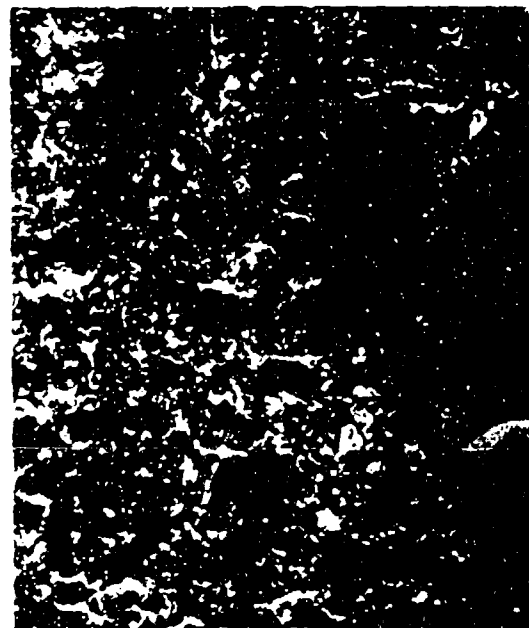
$H_1S_2$   Spec. No. VHS-1   15X
Discontinuous Frosting

FIGURE 5.   MAGNIFIED VIEWS OF DAMAGE ON WEATHERED SPECIMENS
OF SINGLE-LAYER COATING AND TWO-LAYER COMPOSITE
COATING TESTED FOR RAIN-EROSION RESISTANCE

30.

The response of these coating types to high-speed waterdrop impacts is quite different after weathering from their response prior to weathering. When tested prior to weathering, polyurethane coatings gradually develop fatigue cracks which eventually lead to formation of a hole through the coating. At the time the hole forms, the coating shows no sign of wear. This is the failure mechanism of a high-strength material. When tested after weathering, polyurethane coatings develop a surface frosting in a matter of several minutes; short cracks form and coating material breaks away along the edge of the restraining frame almost at once. Presumably a crack forms along the edge of the restraining frame and this leads to the loss of coating material. This is the failure mechanism of a low-strength, relatively nonelastic material.

The change in color of the polyurethane coating material from water white to a bright amber yellow indicates that a fundamental change has occurred in the polymeric material. The change in the mechanism by which erosion occurs indicates that the polymeric material has lost both strength and elasticity. The factors that produce weathering deterioration are oxygen, ozone, ultraviolet light, and humidity. To understand the changes that occurred in the coating material during weathering it would be necessary to go into the chemistry of the urethane polymers. The loss in elasticity suggests a shortening of the coiled polymer chains. Bond rupture can be brought on by ozone addition.

Because polyurethane coatings are currently used to protect radomes from rain-impact damage, the weathering deterioration of these coatings is an area of interest for continued research. The use of antioxidants and of means to reflect ultraviolet light and so prevent it from passing through radome coatings suggest themselves as possible avenues to be explored. Although a transparent topcoat of hard polyurethane does not protect a soft polyurethane undercoat from weathering deterioration, an opaque ceramic topcoat might afford this protection by reflecting rather than transmitting ultraviolet light.

## 2.2.3 Specimens Tested for Sand-Impact Resistance

The rotating-arm device at Bell Aerospace Company can be used to test for high-speed solid-particle-impact erosion as well as for high-speed rain-impact erosion. The rotor to which the specimen is attached is brought up to high velocity and the sand, which enters at a specified rate per minute, is given a velocity normal to the specimen surface. The currently used radome coating known as Astrocoat has been tested with use of airfoil shaped specimens at a rotor velocity of 880 ft/sec (600 mi/hr) and a sand velocity of about 600 ft/sec. For these conditions, the relative impact velocity is 1480 ft/sec. The conditions are not excessively severe because the sand grains bounce off the curved (airfoil shaped) specimens.

In planning the sand-impact tests for flat specimens of the four coating types that were studied, milder conditions were selected both because the specimens were flat so that impacts would occur at normal incidence and because milder conditions should result in a wider spread in performance and, therefore, in a better relative rating of the coating types. The rotor velocity first selected was 733 ft/sec (500 mi/hr) and the sand velocity was that attained in free fall under gravity (15 to 20 ft/sec). The sand admittance rate was the standard two pounds per minute.

Two tests run with these conditions using specimens of single-layer $S_2$ coating resulted in failure of the specimens in 30 seconds and 10 seconds, respectively. Calibration runs were then made at rotor velocities of 365 ft/sec and 440 ft/sec. These resulted in erosion times of 60 minutes and 27.5 minutes, respectively. The latter velocity was selected for use in the tests. Test lifetimes obtained for the four coating types by using these conditions are given in Table 2B on page 28.

It can be seen that the average lifetime of the $H_1S_2$ composite coating is 6.63 minutes longer than the average lifetime of the single-layer $S_2$ coating. However, the maximum difference between highest and lowest value for the $S_2$ coating is 5 minutes and that for the $H_1S_2$ coating is 12 minutes. Use of a statistical test indicated that the difference in the average lifetimes is not significant.

32.

The tested specimens are shown as a group in Figure 4B. They were inspected visually and at low magnification with use of a stereomicroscope. It was observed that the entire face of each of the specimens of $S_2$ coating and $H_1S_2$ coating was abraded. The sand grains ranged in size from 20 to 1,000 microns. The grains that are above 100 microns in size are rough rectangular particles. From Figure 4B it can be seen that sand impact damage is restricted to the low-speed end of a specimen (the specimens have slipped under the restraining frame under the action of centrifugal force). The sand enters in such a way that it only impinges against the low-speed end of a specimen.

The sand-impact damage at the low-speed end of the specimens consists of the development of a network of cracks followed by the breaking away of pieces of coating material between intersecting cracks. A view of the network of cracks on Specimen No. 1 of $H_1S_2$ coating is shown in the upper left picture of Figure 6. A section of the primer coated substrate from which the coating has broken away is visible. A view of the network of cracks on Specimen No. 4 of $S_2$ coating is shown in the lower left picture of Figure 6. The uneroded band along the edge of the specimen was covered by the restraining frame and was protected in this way from sand impacts.

The upper right picture of Figure 6 shows the crack that developed along the restraining frame at the low-speed end of Specimen No. 4 of $S_2$ coating. The $H_1S_2$ specimens that were tested under sand impact at the same velocity showed no evidence of a crack along the restraining frame.

The lower right views of Figure 6 were taken on Specimen No. 4 of $S_2$ coating. They provide evidence that the coating was not worn thin by the sand but that it broke away between intersecting cracks. In the lower of these two pictures the camera is focused on the edge of the specimen which was protected from sand impacts; this view shows the original thickness of the polyurethane coating. A white structure (out of focus) is visible above the coating surface. This is a raised section of
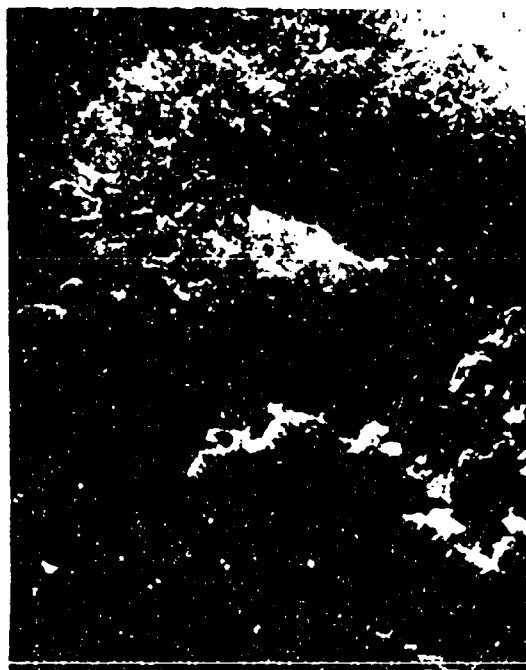
Network of Cracks on $H_1S_2$ Specimen No. 1
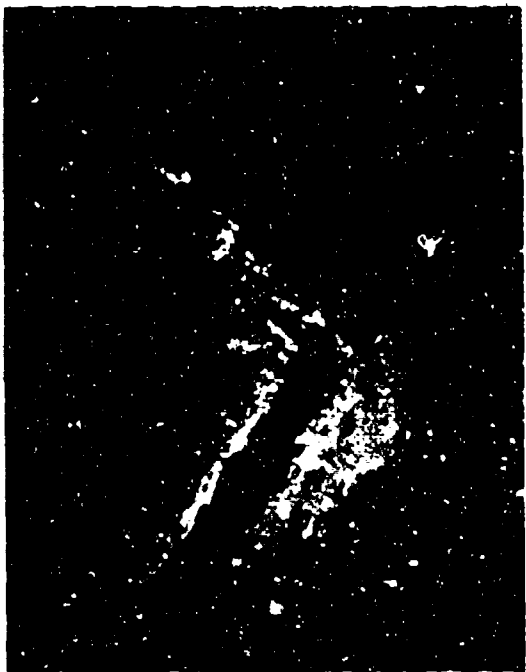
Crack Along Frame on $S_2$ Specimen No. 4

Network of Cracks on $S_2$ Specimen No. 4

Evidence That Coating Is Not Worn Thin

FIGURE 6. VIEWS ON POLYURETHANE COATINGS TESTED FOR SAND-EROSION RESISTANCE

34.

coating that has broken away from the substrate as a result of crack formation by the sand-grain impacts. In the upper picture the light intensity is reduced and the raised section of coating is brought into focus. It can be seen that the loosened coating has not been worn thin by abrasion or by a cutting action of the sand grains; it has simply broken away between intersection cracks.

The evidence that has been presented indicates that for normal impacts of sand grains a polyurethane coating fails by developing cracks. The accumulated cracks form a network. Eventually, pieces of the coating detach between intersecting cracks. The test results do not show a significant difference in resistance to this type of erosive attack for the single-layer $S_2$ coating and the two-layer composite coating $H_1S_2$.

It is noteworthy that, if curved (airfoil shaped) test specimens had been used, the cutting action of the sand grains would have come into play and the mechanism of attack would have been different. It is possible that the hard surface layer of a two-layer composite coating might provide more protection than the single-layer softcoat $S_2$ against erosive attack that involves the cutting or gouging action of the sand grains.

## 2.3 RESULTS OF ROTATING-ARM TESTS AT BRITISH ROYAL AIRCRAFT ESTABLISHMENT

As stated in Section 2.1, three square specimens of each of the four coating types were sent to British Royal Aircraft Establishment, Farnborough, Hants, England, for rain-erosion test after they were inspected with the microscope to insure that they were free of defects. Two additional defect-free single-layer and multilayer specimens were found. These were sent as spares. In addition, six square specimens of multi-layer coating, which had not been inspected for defects, were sent from Olin Research Center where the coating specimens were prepared. All of the specimens that were sent were tested.

The tests were run in five-minute increments of time at a velocity of 500 mi/hr (733 ft/sec) with a one-inch-per-hour rain density, at an impact angle of 90 degrees. Drop size ranged from about 0.5 to 5 mm. The square specimens were mounted on the test device in such a way that the woof fibers of the top glass cloth layer were perpendicular to the direction in which centrifugal force acted on them during the tests. This is the same orientation of the woof fibers as was used in the tests that were run at Bell Aerospace Company (see Section 2.2).

The tested specimens and a report of the test lifetimes that were measured were received from Mr. Roy B. King on June 7. A picture of the tested specimens is shown in Figure 7. The test lifetimes in minutes are listed in order of decreasing size in Table 3; the lifetimes of the multilayer specimens that were not inspected for defects prior to test are marked with asterisks.

It can be seen at a glance that although the single-layer coating $S_2$ and the two-layer composite coating $H_1S_2$ had a single lifetime of 120 minutes and 110 minutes, respectively, their re-maining lifetime values are lower than the lowest lifetime of the five comparable multilayer coating specimens. All three speci-mens of the stress-bumper coating had the same length of lifetime and this lifetime is also lower than the lowest test lifetime obtained for the five comparable multilayer coatings.

LEFT TO RIGHT SINGLE-LAYER $S_2$ SPECIMENS 10 THROUGH 14

LEFT TO RIGHT TWO-LAYER $H_1S_2$ SPECIMENS 7 THROUGH 9

LEFT TO RIGHT MULTILAYER $H_1H_2H_3S_3S_2$ SPECIMENS 15 THROUGH 19

LEFT TO RIGHT STRESS-BUMPER $S_2H_1S_2$ SPECIMENS 20 THROUGH 22

LEFT TO RIGHT MULTILAYER $H_1H_2H_3S_3S_2$ SPECIMENS 1* THROUGH 6*

FIGURE 7. FOUR TYPES OF POLYURETHANE COATING AFTER RAIN-
EROSION TEST AT BRITISH ROYAL AIRCRAFT
ESTABLISHMENT, FARNBOROUGH, HANTS, ENGLAND

37.

# TABLE 3

## DISTRIBUTION OF TEST LIFETIMES OBTAINED AT ROYAL AIRCRAFT ESTABLISHMENT. All lifetimes are in minutes.

| Multilayer $H_1H_2H_3S_3S_2$ | | Single Layer $S_2$ | Two-Layer $H_1S_2$ | Stress Bumper $S_2H_1S_2$ |
|---|---|---|---|---|
| 130 | | | | |
| | *120 | 120 | | |
| | *110 | | 110 | |
| 105 | *105 | | | |
| 95 | | | | |
| 95 | | | | |
| 95 | *95 | | | |
| | *90 | | | 90 |
| | | | | 90 |
| | | | | 90 |
| | *85 | 85 | | |
| | | 85 | | |
| | | 80 | | |
| | | | 70 | |
| | | 60 | 60 | |
| **Average Lifetime** | | | | |
| 104 | *100.8 | 86 | 80 | 90 |
| **Maximum Lifetime Difference** | | | | |
| 35 | *35 | 60 | 50 | 0 |

* All specimens were given microscopic inspection for defects prior to test except those marked with an asterisk. Two of the lifetimes marked with asterisks were for specimens that were mounted with incorrect orientation of woof fibers.

The average lifetimes cannot be used to rate the four coating types for rain-erosion resistance because the differences between the average lifetimes are small in comparison with the scatter in the lifetime values. The fact that the multilayer coating had the highest average lifetime both for the tests run at Bell Aerospace Company and for the tests run at British Royal Aircraft Establishment suggests that it has the highest rain-erosion resistance of these four coating types.

The tested specimens were inspected at low magnification with a stereomicroscope. A summary of the observations for the three modes of failure that were monitored is given in Table 4. Observations made on the multilayer specimens that were not inspected prior to test are given in Table 4 A. The trends in the observations are similar to those made on the specimens tested at Bell Aerospace Company but the extent to which these trends are emphasized is different.

As in the tests run at Bell Aerospace Company, the single-layer $S_2$ coating developed adhesion loss principally in the vicinity of cracks and holes (see upper right view of Figure 8). On the other hand, the two-layer $H_1S_2$ composite coating is characterized by initiation of adhesion loss on protruding woof fibers (see lower right view of Figure 8); this was also characteristic of the $H_1S_2$ coating in the tests run at Bell Aerospace Company (see lower left view of Figure 2). Specimens of multilayer coating $H_1H_2H_3S_3S_2$ tested at Royal Aircraft Establishment and at Bell Aerospace Company showed signs of adhesion loss on protruding woof fibers (see lower left picture of Figure 9) after characteristically long periods of test. The stress-bumper composite coating $S_2H_1S_2$ developed adhesion-loss runners along glass fibers at both testing sites (compare upper left view of Figure 9 with lower left view of Figure 3).

A notable difference in the response of the four coating types to rain-erosion test at the two testing sites is the large number of cracks that developed during the tests at Royal Aircraft Establishment (compare Tables 1 and 4). This may reflect a larger drop-size range at Royal Aircraft Establishment as well as

TABLE 4

RESULTS OF INSPECTION OF COATING SPECIMENS TESTED AT ROYAL AIRCRAFT ESTABLISHMENT

| Spec'm No & Test Time / Type of Failure | SINGLE-LAYER COATING $S_2$ | | | | |
|---|---|---|---|---|---|
| | No. 10 120 min | No. 11 80 min | No. 12 85 min | No. 13 85 min | No. 14 60 min |
| HOLES | 2 large holes; 3 to 4 small | 1 very large hole | 4 large and 1 small near frame | 1 large at frame 4 small isolated | 1 large hole in frame corner |
| CRACKS | 9 isolated cracks | 2 small isolated 2 frame cracks | 11 small isolated cracks | 8 small isolated cracks | 9 small and 1 large isolated |
| ADHESION LOSS | Adhesion loss is associated with cracks and holes and also occurs at one corner of the specimen | Adhesion loss is associated with the frame cracks and hole | Adhesion loss is associated with holes | Adhesion loss is associated with holes | Adhesion loss is associated with holes |

| Spec'm No & Test Time / Type of Failure | MULTILAYER COMPOSITE COATING $H_1H_2H_3S_3S_2$ | | | | |
|---|---|---|---|---|---|
| | No. 15 95 min | No. 16 130 min | No. 17 105 min | No. 18 95 min | No. 19 95 min |
| HOLES | 1 small hole | 1 large hole | 2 holes at frame | 1 large and 1 small hole | 2 large and 3 small holes |
| CRACKS | 2 large and 5 small cracks | 5 large and 3 small cracks | 4 small cracks | no isolated cracks | 11 small cracks |
| ADHESION LOSS | Adhesion loss on protruding woof fibers; it is also associated with the hole and exists in one corner of the specimen | Adhesion loss on protruding woof fibers and associated with the hole and cracks | Adhesion loss on protruding woof fibers and associated with holes | Adhesion loss on protruding woof fibers and associated with holes | Adhesion loss on protruding woof fibers and associated with holes and cracks |

## TABLE 4. Continued

RESULTS OF INSPECTION OF COATING SPECIMENS TESTED AT ROYAL AIRCRAFT ESTABLISHMENT

### TWO-LAYER COMPOSITE COATING $H_1S_2$

| Spec'm No. & Test Time / Type of Failure | No. 7  70 min | No. 8  60 min | No. 9  110 min |
|---|---|---|---|
| HOLES | 1 small hole in frame corner | 1 large hole at frame edge | 2 large holes at frame edge; 1 small isolated |
| CRACKS | 5 large and 4 small cracks | 7 large and 7 small cracks | 5 large and 3 small cracks |
| ADHESION LOSS | Adhesion loss on protruding woof fibers and associated with holes and cracks. Adhesion loss also in one corner of the specimen | Adhesion loss on protruding woof fibers and associated with hole and cracks | Adhesion loss on protruding woof fibers and associated with holes and cracks |

### STRESS-BUMPER COMPOSITE COATING $S_2H_1S_2$

| Spec'm No. & Test Time / Type of Failure | No. 20  90 min | No. 21  90 min | No. 22  90 min |
|---|---|---|---|
| HOLES | 1 large and 4 small holes | 3 small holes | 2 holes at edge of frame |
| CRACKS | 16 cracks that are mostly star shaped | 10 small isolated cracks | 3 cracks along frame; 15 small cracks |
| ADHESION LOSS | Adhesion loss is associated with holes and cracks. There are adhesion-loss runners along glass fibers. | Adhesion loss is associated with holes and cracks. There are adhesion-loss runners along glass fibers. | Adhesion loss is associated with holes and cracks. There are adhesion-loss runners along glass fibers. |

TABLE 4 A

RESULTS OF INSPECTION OF COATING SPECIMENS TESTED AT ROYAL AIRCRAFT ESTABLISHMENT

*MULTILAYER COMPOSITE COATING $H_1H_2H_3S_3S_2$

| Spec'm No. & Test Time / Type of Failure | No. 1 95 min | No. 2 120 min | No. 3 90 min |
|---|---|---|---|
| HOLES | 4 large holes | 1 large hole | 1 large hole |
| CRACKS | 3 large cracks | 3 large and 10 small cracks | 2 large and 4 small cracks |
| ADHESION LOSS | Adhesion loss on protruding woof fibers, at holes and cracks, and along the restraining frame. | Adhesion loss on protruding woof fibers and associated with hole and cracks. | Adhesion loss on protruding woof fibers and associated with hole and cracks. |

*MULTILAYER COMPOSITE COATING $H_1\underline{H_2}H_3S_3S_2$

| Spec'm No. & Test Time / Type of Failure | No. 4 110 min | No. 5 85 min | No. 6 105 min |
|---|---|---|---|
| HOLES | 1 large isolated hole and 2 small holes at cracks | 1 large hole at frame corner and 1 small hole | 1 large hole at frame and 1 small isolated hole |
| CRACKS | 2 small cracks | 3 large and 3 small cracks | 3 isolated cracks; also crack along frame |
| ADHESION LOSS | Adhesion loss on protruding woof fibers, along restraining frame, and at holes. | Adhesion loss on protruding woof fibers and associated with cracks and holes. | Adhesion loss on protruding woof fibers and associated with holes and cracks. |

* These specimens were not given microscopic inspection for defects prior to testing.

$S_2$ Specimen No. 11   7.5X
Effect of Restraining Frame

$S_2$   Specimen No. 13   7.5X
Unimpaired Condition of Primer

$H_1S_2$ Specimen No. 8   7.5X
Cracks Near Edge of
Restraining Frame
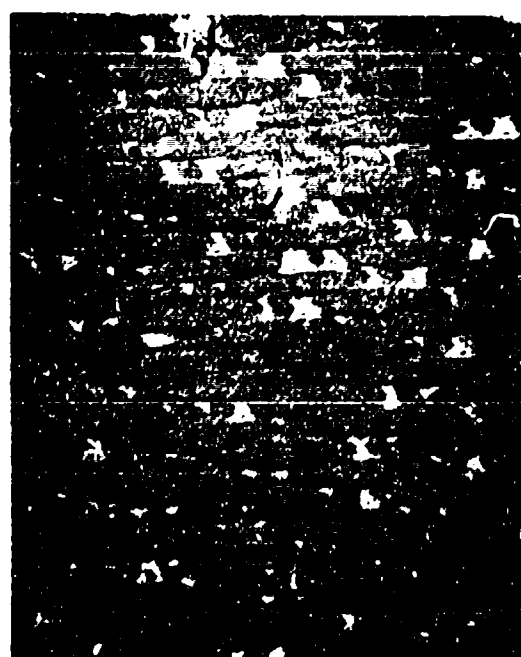
$H_1S_2$   Specimen No. 7   7.5X
Adhesion Loss on Protruding
Woof Glass Fibers

FIGURE 8. MAGNIFIED VIEWS OF DAMAGE ON SINGLE-LAYER COATING AND
TWO-LAYER COMPOSITE COATING TESTED AT BRITISH R.A.E.
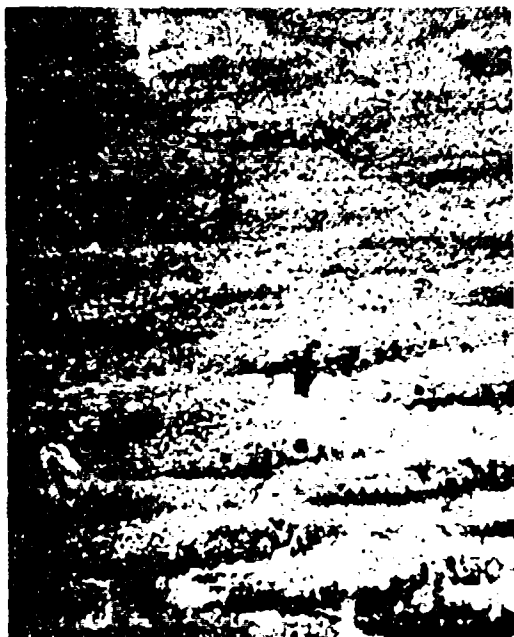
$S_2H_1S_2$  Specimen No. 22  15X
Adhesion-Loss Runners

$S_2H_1S_2$  Specimen No. 20  15X
Crack Formation
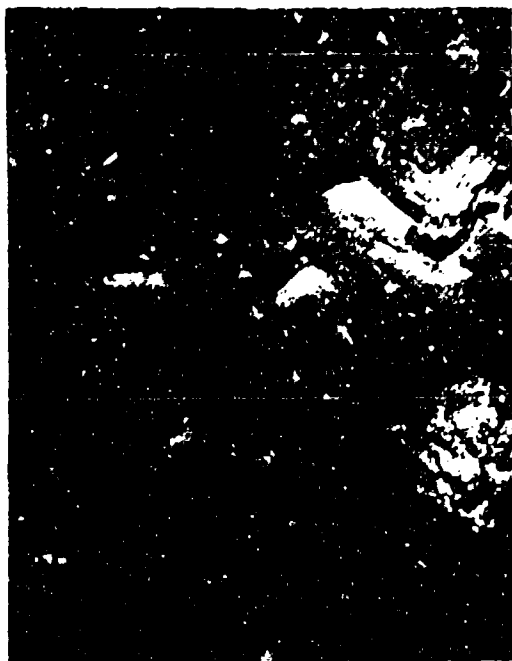
$H_1H_2H_3S_3S_2$  Spec. No. 19  7.5X
Adhesion Loss on Wood Fibers

$H_1H_2H_3S_3S_2$  Spec. No. 1*  7.5X
Effect of Restraining Frame

FIGURE 9.  MAGNIFIED VIEWS OF DAMAGE ON STEEL-PUMICE AND
MULTILAYER COMPOSITE COATINGS TESTED AT LITTLE, F.A.E.

44.

the difference in length of the average test lifetimes for the
coating types obtained at the two testing sites. These are sum-
marized below. That the ratio of lifetimes obtained at the two

| AVERAGE TEST LIFETIMES AND RATIOS OF THE AVERAGE LIFETIMES | | | | |
|---|---|---|---|---|
| Rotor ╲ Coating Type | Single-Layer $S_2$ | Two-Layer $H_1S_2$ | Multilayer $H_1H_2H_3S_3S_2$ | Stress-Bumper $S_2H_1S_2$ |
| Bell Aerospace Comapny | 28.8 min | 49.2 min | 51.0 min | 34.2 min |
| Royal Aircraft Establishment | 86 min | 80 min | 102.3 min | 90 min |
| RAE/BAC Ratio | 3 | 1.6 | 2 | 2.6 |

testing sites varies from 2 to 3 implies that the test at Bell
Aerospace Company was 2 to 3 times as severe as the test at Royal
Aircraft Establishment. The longer test times obtained at Royal
Aircraft Establishment favor fatigue of the coatings under the
pull of centrifugal force and the flow of the drop liquid which
is driven by centrifugal force. This would be expected to result
in the generation and growth of fatigue cracks.

From the tabulation of average lifetimes it can be seen
that the relative ratings of the coatings are

Bell Aerospace
Company        $H_1H_2H_3S_3S_2$, $H_1S_2$ $>$ $S_2H_1S_2$, $S_2$

Royal Aircraft
Establishment  $H_1H_2H_3S_3S_2$ $>$ $S_2H_1S_2$, $S_2$, $H_1S_2$
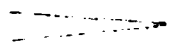
even though these ratings may not be statistically significant
because of the scatter in the data. In these two ratings the
position of the $H_1S_2$ two-layer composite coating is inverted
from that of a leader to that of trailer.

A similar inversion in the rating of the $H_1S_2$ two-layer composite coating was obtained earlier [2] when test lifetimes of airfoil shaped specimens of $S_2$ single-layer coating, $H_1$ single-layer coating, and $H_1S_2$ two-layer composite coating were obtained at Olin Research Center and at Wright-Patterson Air Force Base. The ratings obtained were
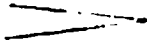
Olin Research Center       $S_2$, $H_1S_2$       $H_1$

Wright-Patterson Air       $S_2$       $H_1$, $H_1S_2$
    Force Base

The test lifetimes obtained at Wright-Patterson Air Force Base, where the testing conditions are mild, were four times as long as the test lifetimes obtained at Olin Research Center. It was surmised [2] that the $H_1S_2$ composite coating failed in fatigue as a consequence of centrifugal force and of unequal yield, which is inherent in the use of airfoil shaped test specimens, during the long test periods at Wright-Patterson Air Force Base because this composite coating has nine mils of high density hardcoat applied over six mils of low density softcoat.

Failure in fatigue as a consequence of centrifugal force and unequal yield are irrelevant as far as the performance of a radome coating is concerned because there is no centrifugal force acting on a radome nor is there a geometry that would lead to unequal yield. What needs to be determined is whether or not the $H_1S_2$ composite coating will fail in fatigue under the stresses imposed by multiple random drop impacts at high speed. In this connection it would be of interest to carry out flight tests with this composite coating as well as tests made with use of the new electrical drop accelerator (see Section 5) because in these tests centrifugal force and unequal yield do not play a role.

In the specimens tested at British Royal Aircraft Establishment, there was also evidence of the effect of the restraining frame that holds the specimen to the rotor. Adhesion loss and crack formation occurred along the frame (see upper left picture of Figure 8 and lower right picture of Figure 9).

## 2.4 LABORATORY TESTS

Parts of a small gas gun, of a system for measuring the incident and rebound velocity of a Nylon sphere fired by the gun, and of a system for measuring the pressure transmitted through a coating struck by the Nylon sphere, which were constructed at Research Institute of the University of Dayton under Navy Contract N00019-71-C-0108, were transferred to Florida Atlantic University for use under Navy Contract N00019-74-C-0063. So the items used in the velocity-measuring and pressure-measuring systems were property of the University of Dayton and had to be replaced with comparable equipment.

An item of the velocity-measuring system, which had to be replaced, was the power supply for the laser light-ladder screens. The replaced items for the pressure-measuring system were the Kistler charge amplifier, the cable and associated adapter that connects the pressure transducer to the charge amplifier, and the oscilloscope on which the amplified charge output of the pressure transducer is displayed after it is converted to a voltage.

During installation and checkout, some parts of the setup were judged to be electrically unsafe. The launch trigger button was rebuilt. A phototransistor trigger circuit was designed and constructed to replace the phototube apparatus used to trigger the oscilloscope. A transformer was used to isolate the light source for the oscilloscope trigger to prevent grounding one side of the 60-cycle power line to the metal mounting framework. All the lines from the high voltage power supply were rebuilt with use of proper connectors and cable. The 5-volt power supply for the instrument panel failed after a few test shots were fired; it was replaced.

The laser tubes were essentially burned out and had to be replaced. The ML310 tubes that had been used were found to be no longer available. The lasers were sent to Metrologic Instrument Corporation in Bellmaur, N.J., where they were modified and refitted with ML610M tubes. The new mechanical dimensions that

resulted from the modification required longer mirrors to form
the laser light-ladder screens of the velocity-measuring system.
Previous specifications for the front surface mirrors called for
aluminum coating No. 756 of Liberty Mirror Division of Libbey-
Owens-Ford Glass Company in Brackenridge, Penn., on twin ground
plate glass. This coating gives a reflectivity of 94 percent
for 6328 $\overset{o}{A}$ light. Two sets of longer replacement mirrors were
purchased from the same company. The replacement mirrors were
made with silver coating No. 950 applied to selected float glass
having a flatness of one fringe per inch; the reflectivity is
97 percent for 6328 $\overset{o}{A}$ light.

To determine the velocity at which a sphere is moving, the
electronic counter should start counting when the Nylon sphere
passes through the first light-ladder screen and it should stop
counting when the Nylon sphere passes through the second light-
ladder screen. After the longer mirrors were installed, a
larger number of reflections of the laser beam occurred with a
consequent loss of light intensity. This may account for the
fact that starting of the counter prematurely by mechanical vi-
bration caused by the action of the solenoid valve became an in-
creasingly frequent occurrence. Rubber sheets placed under the
gun as well as under the laser beam bases corrected this situation
to some extent but did not eliminate it.

The counter is actuated by a phototube that develops a volt-
age when it receives the laser light. If the light intensity
drops, the voltage also drops and the counter is started. By en-
larging the aperature through which the laser light passes to
reach the phototube, the threshhold light intensity needed to ac-
tuate the counter was reduced enough to prevent starting the count-
er by mechanical shock. Increase of the diameter of the aperature
from 1/32 to 1/16 inch, which was the enlargement that was made,
can be expected to reduce the accuracy of the velocity measure-
ment by roughly half of one percent.

The pressure gauge for the compressed gas chamber was intended for use with high gas pressures. The low pressure needed to fire Nylon spheres at a velocity of about 55 ft/sec would not be reproducible with a high degree of accuracy as read from this gauge. To correct this condition without replacing the original gauge, the valve system for the compressed gas chamber was expanded so that a mercury manometer could be introduced to obtain a reproducible gas charge from one Nylon-sphere firing to the next. A picture of the gun in its fully restored operating condition is shown in Figure 10.

To check out the operational repeatability of the gun, ten firings of 3/16-inch Nylon spheres were made at an air pressure of 5.41 psi in the compressed gas chamber. The maximum, minimum, and average velocity for this set of firings were 55.9, 55.4, and 55.6 ft/sec, respectively, using a separation distance of 12 inches between the light-ladder screens and a distance of 7.5 inches between the end of the gun barrel and the mid-point between the light-ladder screens. Consequently, the average velocity produced by this air pressure in the compressed gas chamber represents velocities over a range from 0.3 ft/sec higher to 0.2 ft/sec lower. The chance of obtaining a velocity in this range by setting the air pressure in the compressed gas chamber at 5.41 psi is 0.5 ft/sec out of 55.6 ft/sec or about 0.9 percent. This was regarded as acceptable repeatability.

It was found that the same repeatability can be obtained if a distance of 6 inches between the light-ladder screens is used. However, measurement of the 12-inch distance is subject to less error than measurement of the 6-inch distance. Use of the 6-inch distance could only be justified by a failure of the sphere to pass through the second light screen on rebound to turn the electronic counter off. Such failures were encountered but this state of affairs was corrected by raising the sphere trajectory by 5/16 inch. Consequently, it was unnecessary to resort to use of a 6-inch separation distance between the light-ladder screens.

The experimental procedure used earlier [1,2] to determine both the compressed gas pressure required to deliver an arbitrary

49.
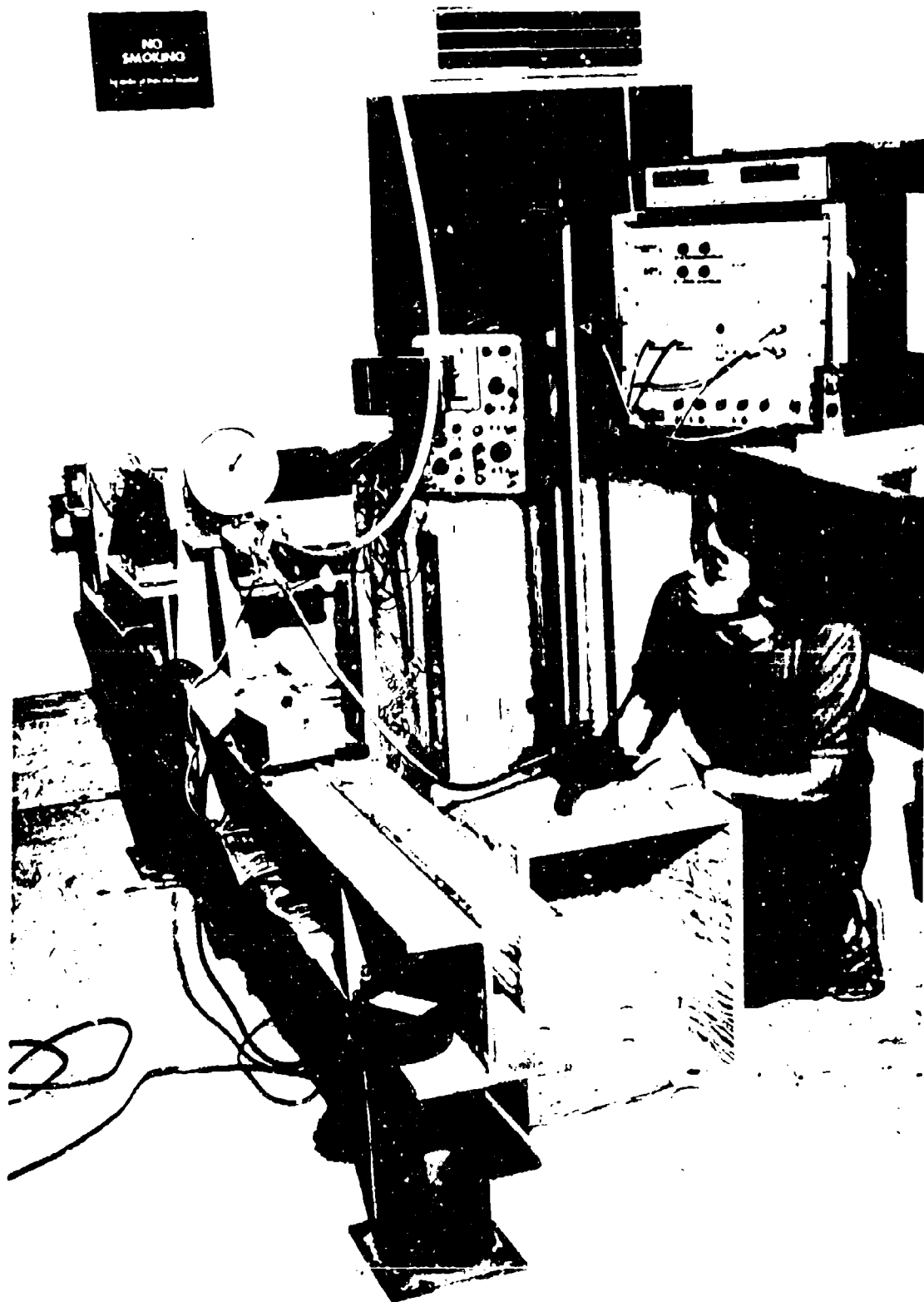
FIGURE 10. SMALL GAS GUN IN FULLY RESTORED OPERATING CONDITION

"standard velocity" at the position of the coating specimen and the loss in velocity due to air drag was followed. The velocity produced at three different distances from the end of the gun barrel to the midpoint of the 12-inch separation between the light-ladder screens was determined for three arbitrary compressed air pressures, namely, 5.0, 5.5, and 6.0 psi. Each velocity identified with one of the specified distances was the average of five good firings. The velocities are plotted against distance in Figure 11. Interpolation between lines for the compressed air pressures that were used makes it possible to select the air pressure needed to produce a given "standard velocity" of impact against a coating specimen placed at any specified distance from the gun muzzle. The slopes of the lines in Figure 11 that were obtained at compressed air pressures of 5.0, 5.5, and 6.0 psi are 1.27, 1.33, and 1.55 ft/sec/ft, respectively. The slopes of the lines give the average loss in velocity due to air drag over the velocity ranges represented.

### 2.4.1 Resilience Measurements

The resilience of each of the four coating types was determined by measuring the incident velocity ("standard velocity") and rebound velocity for firings of 3/16-inch Nylon spheres against specimens of these coating types. Resilience is the quotient of rebound velocity divided by incident velocity.

To make the resilience measurements, the specimen holder that is normally used for making pressure measurements was used. A half inch thick aluminum plate, which contained a hollow so that the piezoelectric gauge would not be in contact with it, was used as a backing for the 20-mil-thick plates to which the coatings are applied. The compressed air pressure used was 5.41 psi which gives a velocity of 55.6 ft/sec at the surface of the coating specimen when the distance between the gun muzzle and coating specimen is 18 inches (see dotted line in Figure 11 ). The distance from the gun muzzle to the first light-ladder screen was 1.5 inches, the distance between the light-ladder screens was
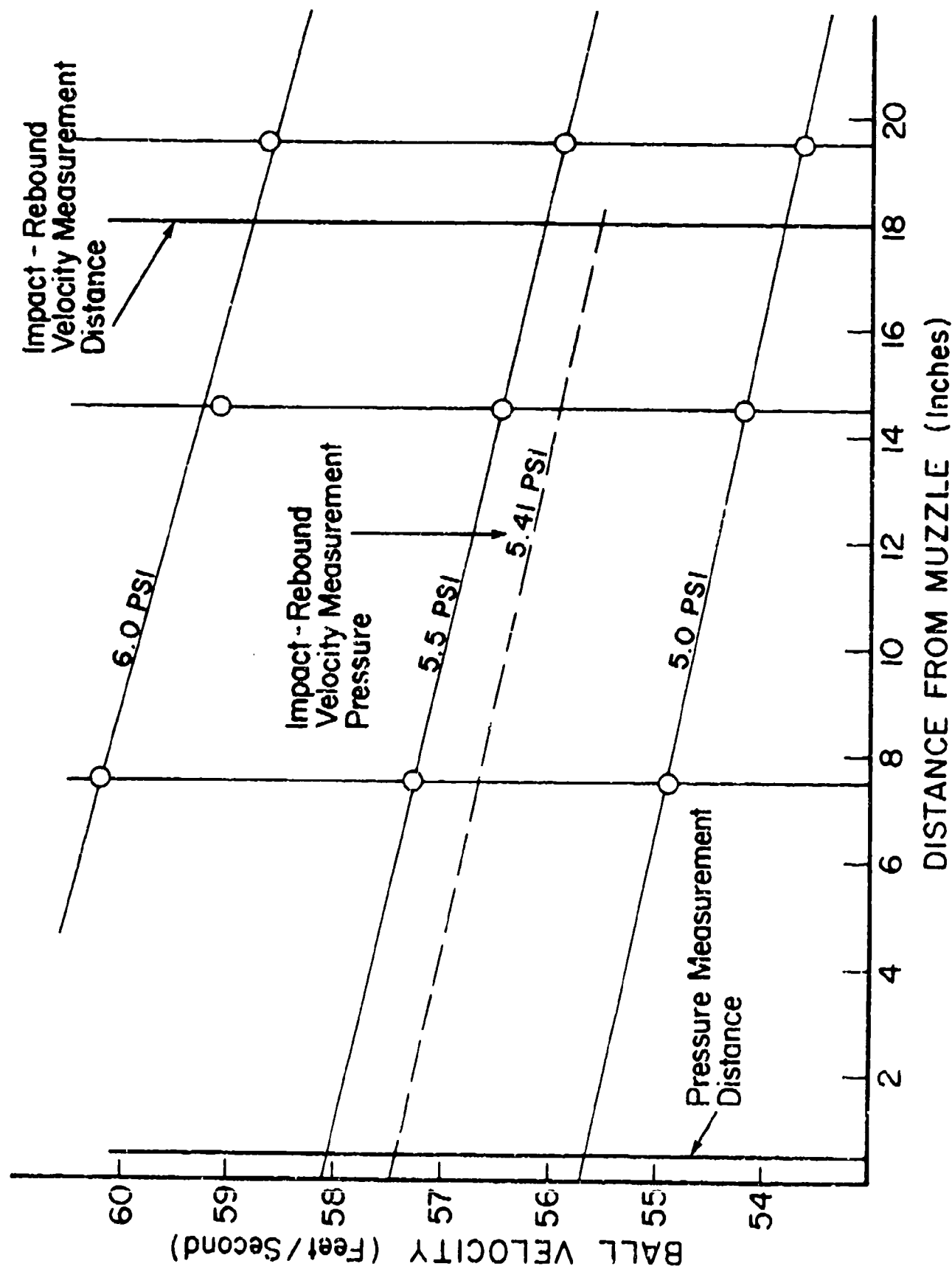
FIGURE 11.  PLOT OF MEASURED VELOCITY AGAINST DISTANCE FROM GUN MUZZLE TO MIDPOINT
BETWEEN LIGHT-LADDER SCREENS

12 inches, and the distance from the second light screen to the specimen was 4.5 inches. Each incident velocity was measured even though the air pressure used was consistently 5.41 psi as far as this could be determined.

There are two known sources of error in the velocity measurements. One of these is that the spheres rebound from the surface of a coating specimen at different angles from one firing to the next. The other is that the velocities are affected by air drag. The size of the error that results from rebound angle can be assessed. In order to obtain a rebound velocity measurement, the rebounding sphere must pass through both light-ladder screens. The most distant one is 16.5 inches from the surface of the specimen. The dimensions of the light-ladder screen are 3 inches by 3.25 inches. If an impinging sphere strikes and rebounds from the edge of the 1-inch-diameter circular specimen, it could yaw by as much as 2 inches in the 16.5-inch travel and still pass through the most distant light screen. In this case, which involves the largest error that could occur, the path length of the sphere would be 16.62 inches instead of 16.5 inches. The increase in path length is 0.73 percent. Because the extent of yaw that occurs for individual firings is not known correction cannot be made for it.

The velocity change caused by air drag involves an error of about 2.5 percent both for the incident velocity and rebound velocity. In correcting for air drag it was necessary to decide whether to use the theoretical air-drag velocity loss per foot of travel or the slope of the dotted line in Figure 11. The velocity of the sphere on reaching the surface of the coating is very close to 55.6 ft/sec. All the velocities that the sphere has had at points between the surface of the coating and the end of the gun barrel were higher than 55.6 ft/sec. The slope of the dotted line in Figure 11 is an average air-drag velocity loss per foot of travel that represents velocities which are for the most part lower than 55.6 ft/sec. On this basis, the theoretical air-drag velocity loss per foot of travel was selected.

The loss in velocity due to air drag can be calculated at any specific velocity from the equation for acceleration, $\alpha$, of a sphere in an airflow which is also applicable to the deceleration of a sphere moving through still air. The equation is [5]

$$\alpha = \frac{C_D \; v_a^2 \; \rho_a \; r^2}{\frac{4}{3} \; \rho_a \; r^3 + \frac{8}{3} \; \rho_s \; r^3} = dV/dt \qquad (2.1)$$

where $V_a$ is the air (or sphere) velocity, $C_D$ is the drag coefficient, $\rho_a$ is the air density, $r$ is the sphere radius, and $\rho_s$ is the density of the material of which the sphere is composed.

Equation (2.1) was used to calculate the loss in velocity due to air drag for a 3/16-inch Nylon sphere moving through still air at a velocity of 55.6 ft/sec. The Reynolds Number for this velocity and sphere diameter is 5155. The drag coefficient for a sphere at this Reynolds Number is 0.4765 by linear interpolation between the values [6] for Reynolds Numbers of 1,000 and 10,000. For this value of drag coefficient, the calculated acceleration is 74.91 ft/sec/sec. The time required to travel over a distance of one foot at a velocity of 55.6 ft/sec is 0.01799 second and the velocity loss due to air drag is 1.348 ft/sec/ft. By comparison the slope of the dotted line in Figure 11 is 1.308 ft/sec/ft.

To facilitate correction of the incident and rebound velocities for air drag, graphs of velocity loss per foot due to air drag were constructed which covered the range of the measured incident and rebound velocities. Measured incident velocities contain the effect of air drag for travel from the gun muzzle to the second light screen because the sphere must reach the second light screen to turn the electronic counter off. However, correction was applied for travel over the distance from the light-screen midpoint to the surface of the specimen. The correction was subtracted from the measured incident velocity. Measured rebound velocities contain the effect of air drag for travel from the surface of the specimen to the first light screen because the sphere, after it rebounds from the specimen, must pass through both light

54.

screens to turn an electronic counter on and off in order to obtain a velocity measurement. In this case, correction was applied for travel over the distance from the specimen surface to the light-screen midpoint.

Resilience is the quotient of the rebound velocity divided by the incident velocity. The measured values of resilience for the four coating types studied are given in Table 5. The dynamic resilience of $S_2$ single-layer coating measured [2] in 1973 was 0.366. The lower value of 0.316 obtained in 1974 suggests that the $S_2$ coating was softer in 1974 than in 1973. This may correlate with the observed formation of adhesion-loss runners. The measured resilience of a hard polyurethane coating $H_1$ is [2] 0.602. It can be seen from Table 5 that the resilience of all three composite coatings is very close to that of the single-layer softcoat $S_2$. This indicates that a large fraction of the energy of an impinging sphere (or waterdrop) is absorbed or dissipated in each of the four coating types studied.

## 2.4.2 Measurements of Pressure Felt at the Substrate Level

To make comparable measurements of the pressure transmitted to the substrate level for each of the four coating types when a Nylon sphere impinges at the "standard" velocity, the quartz crystal in the piezoelectric pressure gauge must be centered with the center of the impact. To insure that this condition will be realized in each firing, the center of the quartz crystal is aligned with the center of the gun barrel just beyond the gun muzzle.

The compressed air pressure needed to give a Nylon sphere the "standard" velocity (55.6 ft/sec) at the time that it emerges from the gun barrel was determined from the plot of Figure 11. It was found to be 5.0 psi. This gas pressure was used for each of the firings made to measure the pressure transmitted to the substrate because it is impossible to strike the center of the quartz crystal in each firing and simultaneously make independent velocity measurements.

TABLE 5

RESULTS OF LABORATORY TESTS ON POLYURETHANE COATINGS APPLIED TO THIN ALUMINUM PANELS

| Coating Type | Thickness mils | Measured Peak Pressure psi | Ball Contact Area sq. in. | Area Ratio A/A_b -- | Max. Pressure at Substrate Surface psi | Time Required to Reach Maximum Pressure microsec | Measured Loading Rate psi/μsec | Resilience at "Standard" Velocity -- |
|---|---|---|---|---|---|---|---|---|
| Single-Layer $S_2$ | 13.7 | 1250 | -- | -- | 9689 | 10.5 | 200 | 0.321 |
|  | 13.8 | 938 | 0.00390 | 5.15 | 7278 | 10.5 | 145 | -- |
|  | 13.8 | 988 | -- | -- | 7665 | 9.5 | 187 | 0.321 |
|  | 14.3 | 1188 | 0.00390 | 5.15 | 9210 | 9.5 | 190 | 0.324 |
|  | 14.5 | 1175 | -- | -- | 9109 | 10.0 | 200 | -- |
|  | 15.4 | 1000 | -- | -- | 7757 | 10.5 | 150 | 0.299 |
| Average | 14.3 | 1090 | 0.00390 | 5.15 | 8451 | 10.1 | 179 | 0.316 |
|  | +1.1 | +160 |  |  | +1238 | +.4 | +21 | +.008 |
|  | -0.6 | -152 |  |  | -1173 | -.6 | -34 | -.017 |
| Two-Layer $H_1S_2$ | 14.3 | 1050 | 0.00363 | 5.54 | 9429 | 10.5 | 187 | 0.288 |
|  | 14.4 | 1330 | 0.00352 | 5.71 | 11935 | 9.5 | 207 | 0.358 |
|  | 15.4 | 1120 | -- | -- | 10055 | 10.0 | 177 | 0.345 |
|  | 15.7 | 1190 | -- | -- | 10682 | 10.0 | 194 | -- |
|  | 16.5 | 1138 | -- | -- | 10217 | 9.5 | 163 | 0.333 |
| Average | 15.2 | 1166 | 0.00358 | 5.62 | 10463 | 9.8 | 176 | 0.331 |
|  | +1.3 | +264 |  |  | +1472 | +.2 | +31 | +.027 |
|  | -0.9 | -116 |  |  | -1034 | -.3 | -13 | -.043 |
| Stress-Bumper $S_2H_1S_2$ | 14.2 | 1318 | 0.00306 | 6.53 | 12568 | 9.5 | 212 | 0.331 |
|  | 14.3 | 1240 | 0.00368 | 5.42 | 12221 | 9.5 | 187 | 0.325 |
|  | 14.7 | 1238 | -- | -- | 12201 | 10.0 | 182 | 0.325 |
|  | 16.4 | 1220 | -- | -- | 12024 | 10.0 | 202 | 0.322 |
| Average | 14.9 | 1254 | 0.00337 | 5.97 | 12359 | 9.8 | 196 | 0.325 |
|  | +1.3 | +64 |  |  | +629 | +.2 | +16 | +.006 |
|  | -0.7 | -34 |  |  | -335 | -.3 | -14 | -.003 |
| Multi-layer | 15.3 | 1288 | 0.00317 | 6.35 | 10887 | 9.5 | 194 | 0.345 |
|  | 16.9 | 1118 | 0.00297 | 6.77 | 9454 | 10.5 | 162 | 0.346 |
|  | 17.1 | 1025 | -- | -- | 8670 | 10.0 | 147 | -- |
|  | 17.3 | 1075 | -- | -- | 9091 | 10.5 | 175 | 0.362 |
|  | 17.3 | 1045 | -- | -- | 8838 | 10.5 | 150 | 0.365 |
| Average | 16.8 | 1110 | 0.00307 | 6.55 | 9388 | 10.2 | 166 | 0.355 |
|  | +.5 | +178 |  |  | +1499 | +.3 | +28 | +.010 |
|  | -1.5 | -85 |  |  | -718 | -.7 | -19 | -.010 |

The charge developed by the quartz crystal as a consequence of the pressure that reaches it is amplified, converted to a voltage, and displayed on an oscilloscope screen. An oscilloscope camera was mounted in front of the oscilloscope screen and a picture of each trace was taken as it appeared. The measured peak pressure is found by measuring the maximum height to which the trace rises above the horizontal time axis. The measured peak pressures were corrected as before [2] for the pressure loss through a 15-mil-thick stainless steel plate which is centered over the quartz crystal. The measured time to reach maximum pressure is found by measuring the distance along the time axis from the point where the trace first rises to the point at which it reaches maximum height. The measured loading rate is found by measuring the angle that the steepest rise of the trace makes with the time axis.

Measured lengths on the photographs of the oscilloscope traces were obtained with use of a pair of dividers and a steel rule. The angle between the steepest rise and the time axis was measured with a protractor that was graduated to 0.5 degree. To obtain loading rate, the tangent of the angle was multiplied by the quotient of the voltage per division on the oscilloscope screen divided by the time per division on the oscilloscope screen. The measured peak pressure, time required to reach peak pressure, and loading rate for the four coating types studied are given in Table 5.

To convert peak pressure to maximum pressure, it is necessary to multiply by the factor $(3/2)(A/A_b)$ where $A$ is the area of the quartz crystal and $A_b$ is the contact area between the Nylon ball and the coating. The area $A$ was calculated from the known diameter of the quartz crystal (0.160 inch). The area $A_b$ was determined by smearing black printer's ink on the surface of the coating specimen and firing a Nylon sphere against it at the "standard" velocity. The diameter of the black spot made on the Nylon sphere was measured with use of dividers and a vernier caliper. The ball contact area was calculated from its measured diameter. The values of maximum pressure transmitted to the substrate for each of the four coating types are given in Table 5.

The thickness of a coating will affect its measured properties. The average thickness of the coatings that were applied to Q-panels from which specimens for the laboratory tests were cut were determined with use of a micrometer caliper. The thickness values are entered in Table 5. It can be seen that the single-layer coating $S_2$, two-layer composite coating $H_1S_2$, and stress-bumper coating $S_2H_1S_2$ were of closely the same thickness but the multilayer coating was about 7 percent thicker.

Inspection of the peak pressures transmitted through the coatings shows that the maximum difference between any two of the coatings is 164 psi. For comparison, the difference between the measured peak pressure transmitted by the single-layer $S_2$ coating and the single-layer $H_1$ coating in 1973 was 555 psi. Similarly, inspection of the maximum pressures transmitted through the coatings shows that the maximum difference between any two of them is 3,908 psi whereas the difference between the maximum pressure transmitted by the single-layer $S_2$ coating and single-layer $H_1$ coating in 1973 was 12,312 psi for the Series 2 coatings and 6,276 psi for the Series 3 coatings. It can be seen that the pressures transmitted through the four coating types as given in Table 5 are roughly the same although small differences exist.

As far as contact area is concerned, the coatings fall in the following order:

$$S_2 \quad > \quad H_1S_2 \quad > \quad S_2H_1S_2 \quad > \quad H_1H_2H_3S_3S_2$$

$$.00390 \qquad\qquad .00358 \qquad\qquad .00337 \qquad\qquad .00307$$

Softest                                                                        Hardest
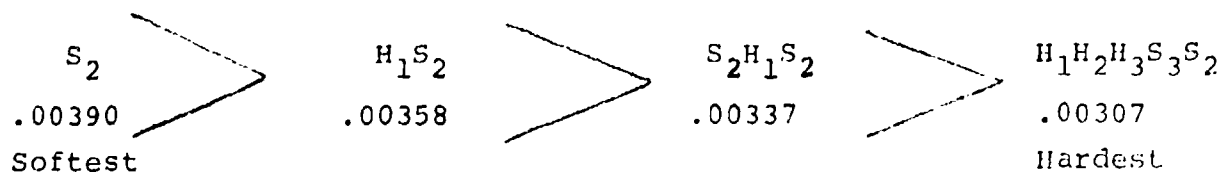
Because the harder a coating is the smaller its impact contact area will be, the above ordering of the coatings is also their ordering as far as hardness or firmness is concerned. This has been indicated below the ordering.

It would be expected that the peak pressure and maximum pressure transmitted to the substrate by the two-layer and multilayer composite coatings might be similar but that, from the standpoint of hardness, the pressure transmitted to the substrate by the multilayer coating might be the larger. The fact that the measured transmitted pressures for the multilayer coating are lower than those for the two-layer coating may reflect the difference in coating thickness, namely, the multilayer coating was 7 percent thicker than the two-layer composite.

The fact that measured peak pressure and maximum pressure for the stress-bumper coating are substantially larger than those for the multilayer coating is surprising. The contact area measurements and the resilience measurements indicate that the stress-bumper coating was softer than the multilayer coating but the pressure measurements indicate that it was harder than the multilayer coating. The pressure measurements are taken through the entire thickness of the coating and may reflect the effect of coating thickness to a greater degree than the contact area measurements or resilience measurements. It is very possible that if the multilayer coating had had a thickness equal to that of the stress-bumper coating its transmitted pressure would have been higher than that of the stress-bumper coating.

In summary, in the light of all the laboratory tests that were performed, it can be said that the differences in the laboratory test results for the four coating types that were studied are small.

## 2.5 RESULTS AND CONCLUSIONS

One of the objectives of the current study was to obtain more data in an effort to establish whether or not a single-layer coating of soft polyurethane $S_2$ has rain-erosion resistance that is better or worse than a composite coating consisting of two or more layers. Considering rain-erosion resistance prior to weathering, the average test lifetime of 28.8 minutes for the single-layer $S_2$ coating obtained in 1974 is significantly lower than the average test lifetime of 49.2 minutes obtained in 1974 for the $H_1S_2$ composite coating. However, the average test lifetime of 48.7 minutes obtained for the single-layer $S_2$ coating in 1973 is the same as the average lifetimes of 51.2 and 49.2 minutes obtained for the $H_1S_2$ composite coating in 1973 and 1974, respectively. A lack of quality control in the preparation of the $S_2$ single-layer coating has prevented realization of this objective of the current study. It can only be concluded that (1) the $S_2$ single-layer coating may or may not perform as well as the $H_1S_2$ composite coating depending upon the quality of the $S_2$ coating.

There is an additional observation of interest in this connection. The average test lifetime of the single-layer hardcoat $H_1$ in 1973 was only 27.5 minutes. Yet when this hardcoat was used in conjunction with the softcoat, which had a test lifetime of 48.7 minutes as a single-layer coating in 1973, the resulting composite coating had a test lifetime of 51.2 minutes which is at least numerically larger than that of the single-layer hardcoat or single-layer softcoat of which it is composed. In 1974, the lifetime of the single-layer softcoat dropped to 28.8 minutes. Yet when this softcoat was used in combination with hardcoat, the test lifetime of which was not determined as a single-layer coating, the resulting composite coating had a test lifetime of 49.2 minutes. This suggests that (2) use of a two-layer composite coating may result in a more stable and predictable average lifetime than use of a single-layer coating. This may or may not be a correct conclusion if both the softcoat and hardcoat are of poor quality; this point has not been demonstrated experimentally.

The average test lifetime of the two-layer composite coating based on the four specimens tested in 1973 and the four specimens tested in 1974 is 50.2 minutes. This is essentially the same as the 51.0-minute average lifetime of the multilayer coating. The maximum spread between the highest and lowest single lifetime for these coating types (34 minutes for the two-layer composite and 30 minutes for the multilayer composite) is also essentially the same. Additional evidence is available from the tests performed at British Royal Aircraft Establishment. In these tests the average lifetime of the multilayer composite coating is 104 minutes with a maximum spread between highest and lowest lifetime of 35 minutes whereas that of the two-layer composite coating is 80 minutes with a maximum spread of 50 minutes. The low average lifetime obtained for the two-layer composite coating may be due to an irrelevant machine effect but this in no way detracts from the excellent performance of the multilayer composite coating. It is concluded that (3) the multilayer composite coating has rain-erosion resistance comparable or superior to that of the two-layer composite coating.

On the basis of theoretical considerations, it was thought that loading rate and impact pressure transmitted to the substrate would be reduced to a greater extent in a stress-bumper (three-layer) composite coating than in a two-layer composite coating because of increased reflection of the impact pressure pulse. It was thought further that this might protect the adhesive bond to the substrate with the result that the stress-bumper coating would outperform the two-layer composite coating. Contrary to expectations, the laboratory test results indicate that the loading rate and transmitted pressure of the stress-bumper coating are higher than those of the two-layer composite coating.

The average test lifetime of the stress-bumper coating was higher than that of the two-layer composite coating for the tests performed at British Royal Aircraft Establishment but was lower than that of the two-layer composite coating for the tests run at Bell Aerospace Company. Adhesion-loss runners were observed on specimens tested at both places. It was also observed that

the stress-bumper coating was susceptible to formation of adhesion-loss runners along the saw cut at the edge of the specimen. This suggests that the large number of reflections of the impact pressure pulse that occur in the stress-bumper coating may result in vibration of the coating with respect to the substrate and that this may bring on adhesion loss with consequent early failure of the coating. If this is the case, the coating may be failing by a different mechanism as a result of the multiple reflections that were introduced in the hope of reducing the loading rate and transmitted pressure that might cause failure of a glass fabric laminate substrate beneath it.

Observed adhesion-loss runners may be the result of a softcoat that is low in isocyanate content so that the acid-type cure that normally occurs at the coating-primer interface may be incomplete. If this is the case, a sticky partially cured layer of softcoat will remain at the substrate level. The effect of this would be that coatings with softcoat adjacent to the substrate would tend to ride off their supporting substrates under the action of centrifugal force during rain-erosion test. Adhesion-loss runner formation was observed for all of the coating types and especially in the case of the stress-bumper coating for the tests run at Bell Aerospace Company; they were observed for the stress-bumper coating for the tests run at Royal Aircraft Establishment.

In the light of these findings, it can only be tentatively concluded that (4) although some reflection of the impact pressure pulse within a coating may be beneficial, it is possible that a threshhold may exist beyond which an increased amount of reflection may be deleterious.

On the basis of observations that were made on tested specimens, (5) one mode of hole formation in polyurethane coatings during rain-erosion test can be identified with isolated cracks that develop. The observations suggest that the isolated cracks originate at the surface of the coating or at defects within the coating and that they grow in depth until they reach the substrate. During the growth of a crack, material can be removed along the crack at the surface of the coating as a consequence of additional impacts or as a consequence of the high-speed flow of accumulated drop liquid over the surface of the coating.

The observations suggest further that when the crack reaches the substrate, adhesion loss occurs in the immediate vicinity of the crack; this may be due to a lifting or movement of the coating. The isolated cracks are generally straight but a certain number of them develop a T structure (referred to as star shaped) as a consequence of formation of a branch. Formation of a branch may or may not require a second impact at the site of the crack. After this degree of weakening has occurred, a subsequent impact at the crack site may induce hole formation.

These observations lead to the conclusion that (6) to be rain-erosion resistant a polymer must resist formation of cracks as a consequence of fatigue in repetitive yielding under random impacts of intercepted rain.

(7) The rain-erosion resistance of polyurethane coatings is strongly reduced by outdoor weathering for ten weeks. The coatings lose strength and become relatively nonelastic. The two-layer composite coating suffered even more weathering deterioration than the single-layer coating.

(8) Both the two-layer composite and the single-layer polyurethane coatings are strongly subject to sand erosion when sand impacts occur at normal incidence. The coatings develop a network of cracks as a result of the sand-impact stresses; coating material detaches between cracks.

## 3. TIME REQUIRED FOR COATING RECOVERY AFTER IMPACT

In comparison with metals and ceramics, rubbers in general are low strength materials. Rubbery coatings used to protect radomes are able to survive high speed rain impingement only because they are able to yield to some extent under the waterdrop blows and in this way reduce the magnitudes of the applied stresses. If a rubbery coating, which has already yielded locally under a waterdrop impact, is struck on essentially the same area by another waterdrop before it has recovered from the first impact, its ability to yield is restricted. In this case, it may not be able to yield enough (that is, to reduce the applied stresses enough) to avert failure. This is why recovery time has been regarded as an important property as far as the ability of rubbery coatings to withstand high speed rain impingement is concerned.

Although the importance of recovery time after impact has been recognized, a technique to measure it has not been developed and the actual recovery times of rubbery coatings used to protect radomes from high speed rain impingement are not known. A technique for measuring the recovery time of a rubbery coating applied to a rigid substrate has been suggested by Mr. Andrew A. Fyall of the British Royal Aircraft Establishment, Farnborough, Hants, England. The suggested method is to fire a spherical mass against the coating and to monitor the disappearance of the crater produced by the impact.

Craters produced by impacts of spheres of different sizes which impinge at different velocities against rubber sheets that have different thicknesses can be expected to recover within different time intervals. To make this method as meaningful as possible as far as high speed rain erosion of coatings is concerned, the spherical mass should exert a pressure comparable to that exerted by a waterdrop that impinges at a velocity close to aircraft flight velocities, that is, at about 500 mi/hr (733 ft/sec) and the thickness of the rubber sheet should be about 0.015 inch.

64.

The impact of a 3/16-inch Nylon sphere at about 55 ft/sec was used as a "standard impact" in laboratory determinations of coating resilience and of pressure transmitted through a coating [1,2]. The velocity of 55 ft/sec was found by trial to be the highest velocity that could be used without producing permanent deformation or set in a 15-mil-thick polyurethane coating as the result of impact of a 3/16-inch Nylon sphere. On this basis it was thought that this velocity for a Nylon sphere may produce about the same impact pressure as that produced by a waterdrop at 500 mi/hr (733 ft/sec). An initial study of the corresponding velocities for equal pressure between Nylon sphere impacts and waterdrop impacts is described in Section 4 of this report.

In the first work that was done on the recovery time of rubbery coatings, the small gas gun that was used to fire Nylon spheres at the University of Dayton Research Institute [1,2] had not yet been received, installed, or brought into operating condition at the Florida Atlantic University. It was necessary to simulate the "standard impact" with use of a freely falling steel sphere. To do this it was necessary to know the fall height that must be used for the sphere.

To establish what the correct fall height of the sphere should be, the corresponding velocity for equal pressure between a Nylon ball impact at 55 ft/sec and a steel sphere impact was calculated. Hertzian equations for impact of a solid sphere against a planar solid are available [2]. The pressure $P_N$ developed when a Nylon sphere impinges against a planar solid having elastic modulus $E'$ is given by

$$P_N = 0.9025 \left[ (E_N E')^4 \; \rho_N v_N^2 \; / \; (E_N + E')^4 \right]^{1/5} \qquad (3.1)$$

where $E_N$ is the elastic modulus of Nylon, $\rho_N$ is the density of Nylon, and $v_N$ is the impact velocity of the Nylon sphere.

## TABLE 5

MATERIAL PROPERTIES NEEDED TO CALCULATE CORRESPONDING VELOCITIES

| Material | Bulk Plane-Wave Velocity, c | Density, $\rho$ | Acoustic Impedance, z $z = c\rho$ | Thin Rod Plane-Wave Velocity, C | Elastic Modulus, E $E = c^2\rho$ |
|---|---|---|---|---|---|
| | cm/sec | g/cm$^3$ | g/sec·cm$^2$ | cm/sec | g/sec$^2$·cm (dynes) |
| Nylon 6-6 | [a]$2.62 \times 10^5$ | [a]$1.11$ | $2.91 \times 10^5$ | [a]$1.8 \times 10^5$ | $3.60 \times 10^{10}$ |
| Plexiglas | [b]$2.68 \times 10^5$ | [b]$1.2$ | $3.22 \times 10^5$ | [b]$1.8 \times 10^5$ | $3.89 \times 10^{10}$ |
| Steel 1& C hardened | [a]$5.854 \times 10^5$ | [a]$7.84$ | $45.9 \times 10^5$ | [a]$5.07 \times 10^5$ | $201.5 \times 10^{10}$ |
| Water distilled | [a]$1.498 \times 10^5$ | [a]$0.998$ | $1.50 \times 10^5$ | ------ | ------ |

a   CRC Handbook of Chemistry and Physics, 49th Edition 1968-69

b   J.R.Frederick, Ultrasonic Engineering, John Wiley and Sons, Inc.  New York, 1965
    See page 363.

Similarly, for a steel sphere,

$$P_s = 0.9025 \left[ (E_s \, E')^4 \, \rho_s \, v_s^2 \, / \, (E_s + E')^4 \right]^{1/5} \quad (3.2)$$

where $E_s$ is the elastic modulus of steel, $\rho_s$ is the density of steel, and $v_s$ is the impact velocity of a steel sphere.

The impact velocity that a steel sphere must have in order to impose the same pressure as that produced by a Nylon sphere impact at any arbitrary velocity can be found by equating Eqs. (3.2) and (3.1). On equating these equations, raising both sides to the fifth power, and taking the square root of both sides, one obtains the expression

$$v_N = (E_s/E_N)^2 \left[ (E_N + E') \, / \, (E_s + E') \right]^2 \, ( \, \rho_s / \, \rho_N)^{1/2} \, v_s .$$

$$(3. \; )$$

The elastic modulus can be calculated from the expression $E = c^2 \rho$ where $C$ is the speed of sound in a rod or bar. Using the data given in Table 2, one finds that

$$v_s = 0.0903 \, v_N \quad (3.4)$$

when the impacts occur against a Plexiglas plate.

The effective elastic modulus of a soft polyurethane rubbery coating applied to an aluminum panel was found [2] to be 78070 psi ($0.5383 \times 10^{10}$ dynes/cm$^2$). For a planar solid having this modulus of elasticity one finds that

$$v_s = 0.286 \, v_N \quad (3. \; )$$

so that the velocity of a steel sphere that would correspond to the standard velocity of about 55 ft/sec is 16 ft/sec. A velocity of 16 ft/sec would be acquired by a steel ball in falling through a distance of four feet if the free-fall velocity is taken to be $(2gh)^{1/2}$ where $g$ is the acceleration due to gravity and $h$ is the height of fall.

## 3.1 CRATER LIFETIMES BY DIRECT OBSERVATION

Some preliminary firings to make a feasibility test of the
proposed method of measuring recovery time of a rubbery coating
were made by Mr. Andrew J. Piekutowsky at the Research Institute
of the University of Dayton. Nylon spheres that were 3/16 inch
in diameter were fired with use of a small gas gun against both
a soft and a firm polyurethane coating (nominal coating thickness
15 mils) at a velocity of 55 ft/sec. A Fastax camera was used
to monitor the disappearance of the impact crater. It was found
that craters produced in the coatings by the firings were still
visible after the 100-foot strip of film had passed through the
camera. The framing rate was 1250 per second as indicated by tim-
er marks at the edge of the film.

It was not known if this relatively slow recovery is a char-
acteristic of polyurethane coatings only or a characteristic of
coatings of other rubbery materials as well. To obtain more in-
formation, an attempt was made to monitor the recovery of craters
formed by steel sphere impacts in a thin sheet of natural rubber
(dental dams with a nominal thickness of 13.5 to 15 mils) that
was bonded to an aluminum plate with Eastman 910 cement. This
experiment was performed before the required fall height for the
sphere was calculated; the fall height used was about one foot
which results in an impact velocity of eight feet per second.

The impacts were photographed with a Fastax camera made
available for the purpose in the Mechanical Engineering Depart-
ment of the University of Miami, Coral Gables, Fla., through the
courtesy of Dr. Harry Wiseman. The framing rate for the Fastax
camera was 1250 per second. This is the lowest framing rate that
can be obtained with a Fastax camera without changing to the use
of direct current. Plus X reversal film supplied by Dr. Wiseman
was used. Three different impacts were photographed. On in-
spection of the films after development, they were found to be
dark; nevertheless, the impact incident was located on each of
two films. No crater formed as a result of the impact could be
seen in either film.

The study was carried further with use of a moving picture camera capable of a frame rate of 64 per second. The first successful attempt to observe the disappearance of an impact crater in a thin sheet of natural rubber that was bonded to an aluminum plate was one for which the surface of the rubber was rendered highly reflective by vapor deposition of aluminum. The fall height of the 5/16-inch steel sphere that was used to produce the crater was 44 inches. Enlarged prints were made of several frames from this film and the average diameter of the impact mark was measured. Immediately after sphere rebound the average diameter of the mark was found to be 0.081 inch. After a time lapse of 20.2 seconds, which was essentially the total time photographed, the average diameter of the mark was found to have decreased to 0.066 inch. The average diameter of the mark as measured on the rubber sheet itself a week later was 0.039 inch.

Attempts made to reproduce the data obtained from this film were unsuccessful until the angle at which the light struck the aluminized surface of the rubber sheet was reduced. Reduction of the angle at which the surface of the rubber was lighted had the effect of throwing depressions, such as the impact crater, into shadow. Pictures of the crater are not shown because the small effect would be lost in reproduction. The distance through which the 5/16-inch steel sphere fell was 49 inches. It was seen that 20 seconds after the impact occurred the circular shadow, which marked the existence of a depression at the point where the steel sphere struck, had disappeared. At the end of 26 seconds of elapsed time, the shadow reappeared. This suggests that recovery of the rubber that was compressed is complicated by vibration.

This film was studied further in an effort to determine if the cycle of appearance and disappearance might be less than 20 seconds. The film was run slowly through a film viewer. At least one observer was able to perceive a cycle of about eight frames. For frames at 1/64-second intervals, eight frames would be equivalent to 0.125 second. A difficulty in this procedure

is that the viewer sees only one frame at a time so that comparison is based on memory. To overcome this difficulty, enlarged permanent prints were made of eleven consecutive frames at the start of this film using the microscope with transmitted light. The micrographs were mounted in chronological order to facilitate inspection. Again, there seemed to be some dimming of the crater about eight frames after the impact occurred. The difference between successive prints, however, is so small as to be at the threshhold of perception. The result is that no conclusive statement with regard to the length of the cycle can be made on the basis of the evidence available.

Other avenues to explore are first the use of thicker rubber sheets so that the impact crater will be more pronounced and secondly the use of other techniques to indicate the disappearance of the crater. Sheets of natural rubber and of neoprene that are 0.062 inch thick were ordered. This provides a factor of four in the thickness of the rubber sheet.

The thick rubber sheet was bonded to aluminum panels with Eastman 910 cement. Panels of double thickness were also made by fastening the second thickness of rubber sheet to the first layer. The second layer was bonded to the first layer only around the perimeter to avoid hardening the rubber with the cement. A vapor deposit of aluminum was applied. Because only the roughing pumps were operative, air pressure in the chamber for the vapor deposition was not as low as should be used. A consequence of insufficiently low air pressure is that the vapor deposits are rough. Moving pictures at the rate of 64 frames per second were made of steel-sphere impacts against these rubbery sheets. The fall height of the sphere was 49 inches. Only two of the moving pictures that were made were considered good. Inspection of these films with a moving picture projector failed to yield the information sought. No noticeable deformation of the rubber as a result of the steel sphere impact was observed.

71.

## 3.2 EXPLORATION OF THE POSSIBLE USE OF THE PHOTOELASTIC TECHNIQUE

Whether or not the photoelastic technique is feasible for indication of recovery time of opaque rubbery coatings depends upon the depth of photoelastic material that must be deposited over the opaque coating in order to see color bands while the impact crater exists. Use of the Pythagorean theorem and the maximum diameter (0.081 inch) of the crater formed on an aluminized rubber sheet by impact of a 5/16-inch steel sphere (see Section 3.1) indicates that the depth of the dimple formed in the rubber coating is about 0.005 inch or five mils. If the depth of photoelastic material required to see the color bands around a crater is a substantial fraction of the 5-mil depth of the dimple in the rubber, the thing measured would be the recovery time of the photoelastic material rather than the recovery time of the rubber.

To investigate the possibility of using the photoelastic technique to measure the time required for a rubbery coating to recover after impact, four small thin sheets of natural rubber were bonded to an aluminum plate with use of Eastman 910 cement. A photoelastic material (PSO-2) obtained from Photolastic Incorporated at Malvern, Penn., was sprayed onto the four small sheets from an aerosol container. Different thicknesses were built up on the four rubber sheets; the thicknesses ranged from 0.7 mil to 2.7 mils.

The recommended curing procedure for the PSO-2 material called for four to six hours at $150^{\circ}F$, 30 minutes at $250^{\circ}F$ and 30 minutes at $300^{\circ}F$. It is not possible to carry out the last two steps of this curing procedure for an application in which the PSO-2 material is deposited over natural rubber because the temperature above which natural rubber should not be put into continuous use is $175^{\circ}F$. To avoid deterioration of the natural rubber sheet, the time-temperature effect was invoked; the PSO-2 material was cured for seven hours at $150^{\circ}F$.

After cure, the PSO-2 coating was found to be only semitransparent and the coating surface was found to be rough. An

attempt was made to induce formation of color bands in these coatings by pressing them with a hollow glass tube. None of the thicknesses of PSO-2 photoelastic material was found to develop color bands.

Photolastic Incorporated was consulted with regard to this negative result. It was learned that about a 20-mil thickness of the PSO-2 photoelastic material would be required in order to see color bands. On the basis of this information, further exploration of the photoelastic technique for use in measuring recovery time of thin rubbery coatings after impact was abandoned because the thickness of photoelastic material required is too great.

It was suggested by Dr. R.O.Case of the Mechanical Engineering Department of the Florida Atlantic University that, if the recovery time of sufficiently thick coatings of a series of various photoelastic materials were to be determined, the unknown recovery time of an opaque rubbery coating could be approximated by comparing its mechanical properties with the mechanical properties of the various photoelastic materials in the series.

73.

## 3.3 EXPLORATION OF THE POSSIBLE USE OF THE MOIRE TECHNIQUE

Use of the Moire technique hinges upon the feasibility of applying grid lines that an impinging solid sphere cannot wipe off to the surface of a rubbery coating.

### 3.3.1 Bondable Grids

Bondable grids are available from Photolastic Incorporated. They can be cemented to various materials. The total thickness of grid plus bonding cement was estimated to be about 0.003 inch. The possible use of such grids was considered to be worth exploring. The 0.081-inch diameter of the crater formed by a 5/16-inch steel sphere (see Section 3.1) after a free fall of 44 inches would be crossed by 16 grid lines of a 200-line-per-inch grid for which the spacing between lines is 0.005 inch. Two 200-line-per-inch bondable Moire grids and the recommended adhesive for bonding them were purchased from Photolastic Incorporated.

Attempts were made to bond these grids to thin natural rubber sheets that were fastened to aluminum plates with Eastman 910 cement. In the first attempts, the recommended adhesive was used. If the adhesive was used in 50-50 ratio with the hardener supplied with it and cured at room temperature for the recommended time under the recommended pressure, the bond between the grid and the natural rubber sheet was found to fail when an effort was made to remove the protective cover from the grid. The same result was obtained when 40 parts of the adhesive were mixed with 60 parts of the hardener and cured under the recommended pressure at about $104^{C}F$ for 22 hours in an oven. It was concluded that the recommended adhesive does not form a sufficiently strong bond to natural rubber to permit its use in bonding a grid to a natural rubber sheet

Attempts were then made to bond a grid to the rubber sheet by using Eastman 910 cement as the adhesive. In one attempt a large part of the grid was successfully bonded to the rubber. In the other attempt, when the protective cover was lifted from the grid the strength of the adhesive bond was greater than the

cohesive strength of the rubber and the rubber pulled out with the grid. Even in the case of the successful attempt, use of Eastman 910 cement was considered to be undesirable because it hardened the surface of the rubber.

To be able to bond grids to rubber sheets successfully with use of a flexible adhesive, further experimentation must be carried out to determine the proper adhesive and application conditions. Further effort in this direction was deferred in favor of attempting to stamp a grid on the surface of the rubber.

### 3.3.2 Grids Stamped on the Surface of a Rubber Sheet

The idea of making a metal stamp to impress grids on rubber coatings and sheets was suggested by Mr. George Haughton of Aeromark Incorporated, Boca Raton, Fla. On consulting with a photoengraving shop it was learned that a 200-line-per-inch grid has a spacing close to that of a halftone. It is so small that a metal stamp cannot be made of it. The possibility of using a coarser grid was then considered. A grid of 50 lines per inch has a 0.020-inch spacing between lines. An impact crater having a diameter of 0.081 inch (see Section 3.2) would be crossed by four lines of a 50-line-per-inch grid. This is about the limiting coarseness that a grid can have to be useful in the application of determining the recovery time of a rubber.

Photolastic Incorporated does not carry a grid master that is coarser than 200 lines per inch. A grid of 50 lines per inch was drawn on paper by Mr. Haughton. It was photographed to obtain the negative and a metal stamp having 50 lines per inch was made with use of the negative. With use of this metal stamp it was found possible to apply grids of yellow ink to thin sheets of natural rubber and polyurethane that were bonded to aluminum plates. It was also found possible to impress this grid in a very thin vapor deposit of aluminum on such a rubbery coating if the grid stamp was first pressed against a flat glossy surface to which a sticky substance had been applied.

75.

Moving pictures at a rate of 64 frames per second were taken of impacts of steel spheres against ink grids impressed on thin layers of natural rubber and polyurethane. In each case, the impact was that of a 5/16-inch steel sphere after free fall through 49 inches. In each case the thickness of the rubber sheet or coating, which was either bonded or applied to an aluminum supporting plate, was about 0.015 inch.

The pictures shown in Figure 12 show an impact against a yellow ink grid that was stamped on a polyurethane coating. The two streaks that appear in the picture of the impact identify the location of the impact area; the streaks were produced by reflections of light from the moving steel sphere. Yet in the indicated area no identifying mark can be seen that was not there before the impact occurred and measurements on the grid lines before and after the impact fail to show a difference that could be associated with deformation caused by the impact.

The views shown in Figure 13 at two different magnifications are of a steel sphere impact against a thin sheet of natural rubber that was stamped with a grid of yellow ink. The white streak in the picture of the impact identifies the location of the impact area. The views shown in Figure 14 are of a steel sphere impact against a thin natural rubber sheet which was first given a vapor deposit of aluminum and then had a grid imprinted in the deposit of aluminum. The rebounding steel sphere can be seen in the picture of the impact. The deformation produced by the impact was still visible after 60 seconds but it may consist of a permanent disturbance of the vapor deposited aluminum. No information regarding recovery time of the rubber sheet was obtained from either of these films.

A final effort to use the Moire grid technique was made with sheets of natural rubber and neoprene that were 0.062 inch thick in the hope that the crater formed would be deeper and the deformation of the grid would be more pronounced. Moving pictures taken of steel-sphere impacts against these sheets yielded no more information when viewed with a motion picture projector than those of steel-sphere impacts against thin sheets of natural rubber and polyurethane.
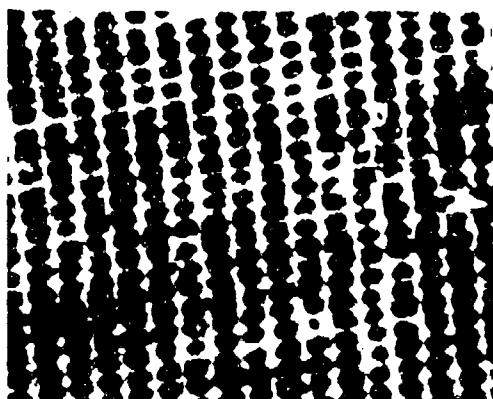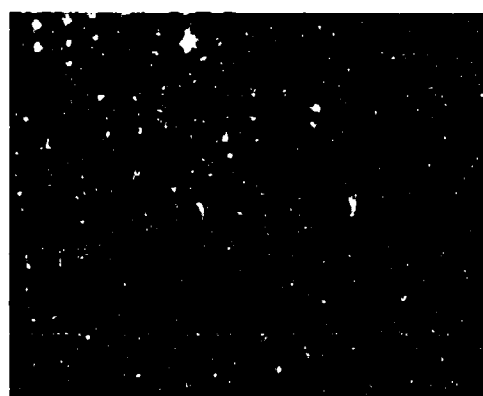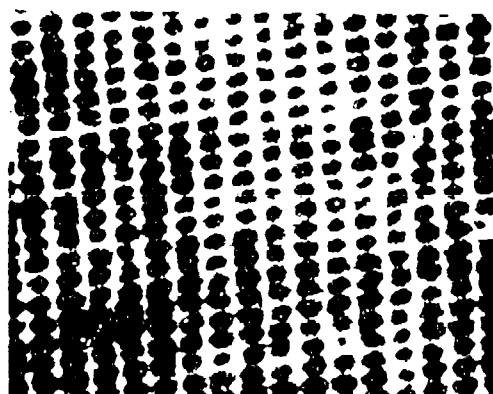
1/64 sec before impact
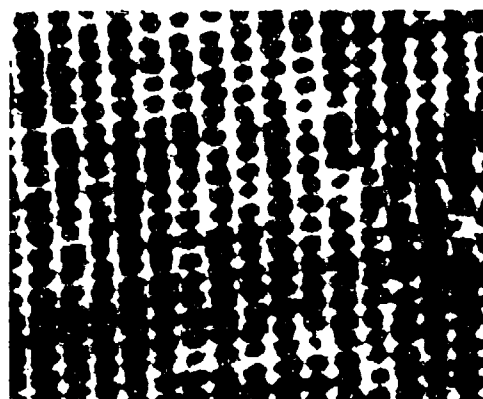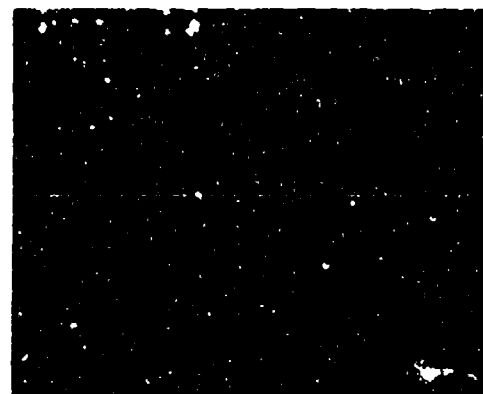
10 sec after impact
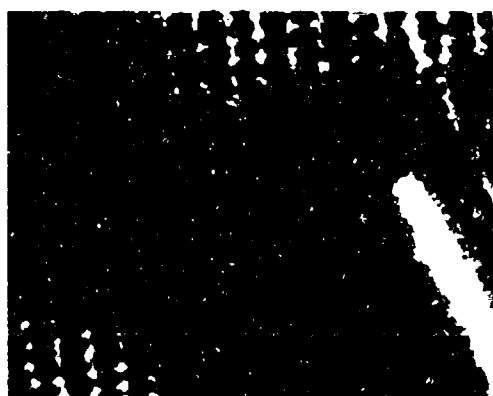
impact

40 sec after impact

1/64 sec after impact

60 sec after impact

FIGURE 12.   IMPACT OF A STEEL SPHERE AGAINST A POLYURETHANE
             COATING THAT WAS STAMPED WITH A GRID OF INK

77.

## 3.4 EXPLORATION OF THE POSSIBLE USE OF AN ELECTRICAL TECHNIQUE

It was suggested by Dr. James B. Davidson of the Ocean Engineering Department that the recovery of a crater formed in a rubber sheet by an impact might be monitored by means of a change in capacitance of the rubber at the point of impact. The feasibility of using this technique was explored by Dr. Peter J. Graham of the Electrical Engineering Department.

The basis of the proposed scheme is to plate a small area (a few square centimeters) of the coating with a thin conducting film (preferably silver or gold) by vacuum deposition. The film must be thick enough to form a good conducting surface but not so thick as substantially to change the mechanical properties of the coating. The minimum thickness depends primarily upon the smoothness of the surface of the thin rubber sheet or coating. Because the conducting film is to serve as one plate of a capacitor, the capacitance of which is to be measured at a frequency of the order of a megahertz, all of the current carried by the film will be essentially on the outer surface due to skin effect.

The other plate of the capacitor is the metal supporting plate of the rubber sheet or coating; the coating itself serves as the dielectric. When the coating is depressed by impact of a Nylon ball, there will be a slight increase in the capacitance as a consequence of the decrease in separation of the plates under the impinging sphere. The capacitance will continue to change with time until the coating relaxes into its final equilibrium position.

The method suggested to detect the change in capacitance is to make the metal plated coating and its metal supporting plate a part of the L-C circuit that controls the frequency of an oscillator. This has been done using a 1/16-inch-thick sheet of neoprene that was bonded to an aluminum plate with Eastman 910 cement and plated with a deposit of aluminum; the vapor deposit of aluminum covered an area of about four square centimeters. If this assembly parallels the L-C circuit of a 1 MHz Colpitts oscillator, the frequency change that occurs

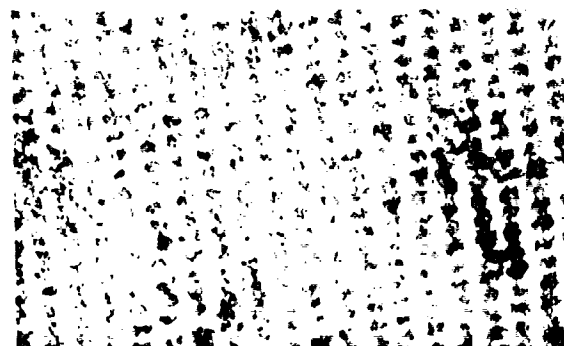1/4 second before impact



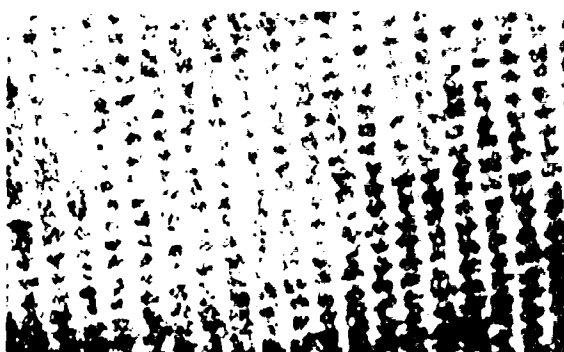impact



1/64 second after impact
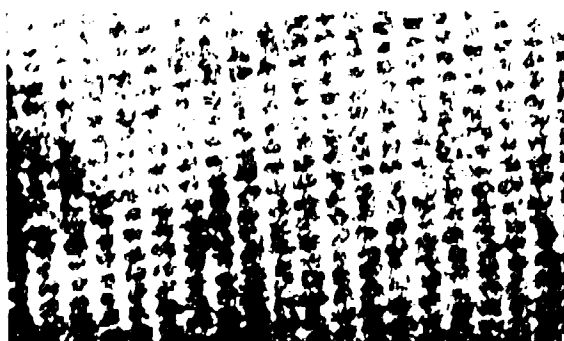


20 seconds after impact



20 seconds after impact
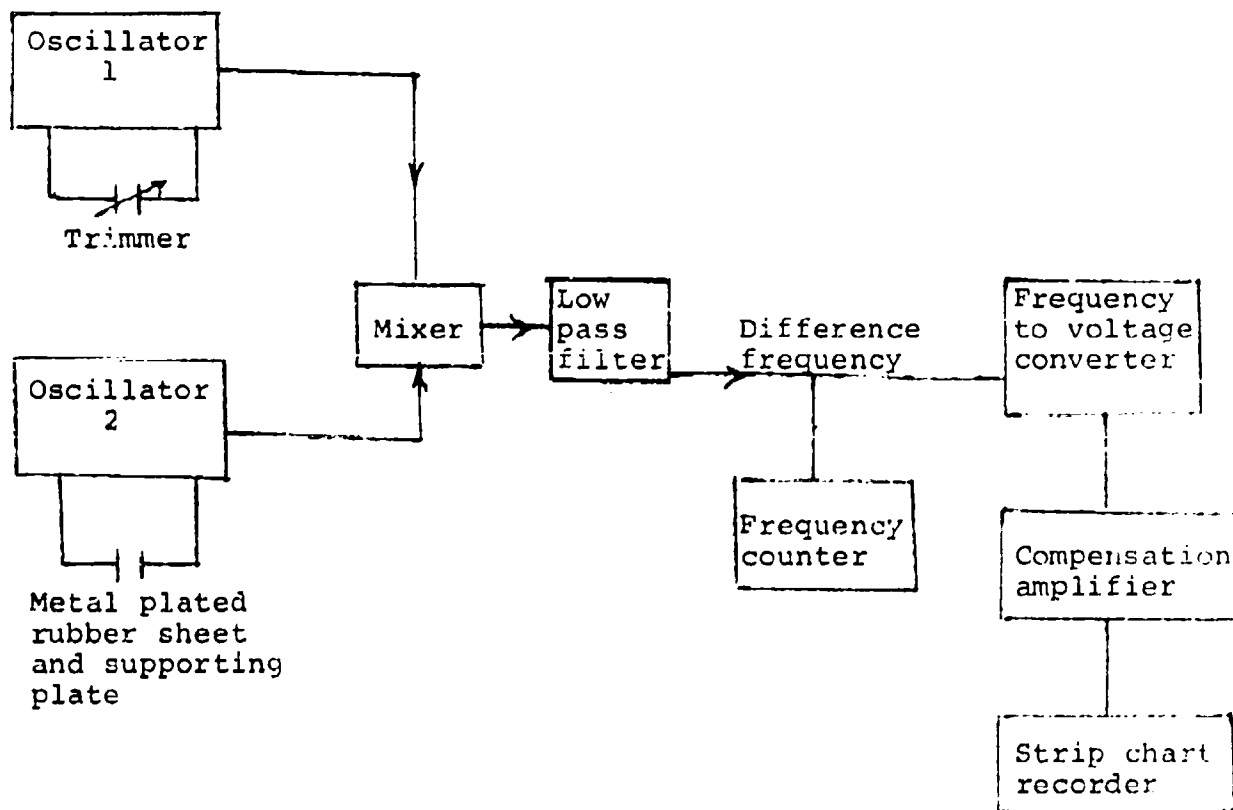
1/64 second before impact

impact

1/64 second after impact

20 seconds after impact

IMPACT AGAINST YELLOW INK GRID ON NATURAL FUR

78.

when the metal plated surface of the rubber is depressed with
a plastic probe was found to be of the order of 0.001 to 0.01
percent. It is considered feasible to monitor a frequency
change of this magnitude.

A system by means of which the small observed change in
frequency can be monitored is shown in the following functional
diagram. Care must be taken to make the oscillators identical

```
 ┌──────────┐
 │Oscillator│
 │    1     │──────────────┐
 └──────────┘              │
   └──┤├─┤                 │
    Trimmer                ▼
                    ┌───────┐  ┌──────┐                      ┌──────────┐
                    │       │  │Low   │   Difference         │Frequency │
                    │ Mixer │─▶│pass  │──▶frequency ──────── │to voltage│
                    │       │  │filter│                      │converter │
 ┌──────────┐       └───────┘  └──────┘                      └──────────┘
 │Oscillator│          ▲            │                             │
 │    2     │──────────┘            │                        ┌──────────┐
 └──────────┘                       ▼                        │Compensation│
   └──┤├─┘                   ┌──────────┐                    │amplifier │
                             │Frequency │                    └──────────┘
 Metal plated                │counter   │                         │
 rubber sheet                └──────────┘                    ┌──────────┐
 and supporting                                              │Strip chart│
 plate                                                       │recorder  │
                                                             └──────────┘
```

both with regard to component values and component placement. A
matched transistor pair in the same case (a 2N3251, for example)
is suggested; use one of the pair for each oscillator. This will
subject both oscillators to approximately the same frequency drift
due to temperature changes

Preparing the system for a given sample of rubber sheet or
coating bonded to a supporting plate would require that, after
the sample of rubber sheet is connected, the trimmer capacitor
of Oscillator 1 be adjusted for a difference frequency appropriate
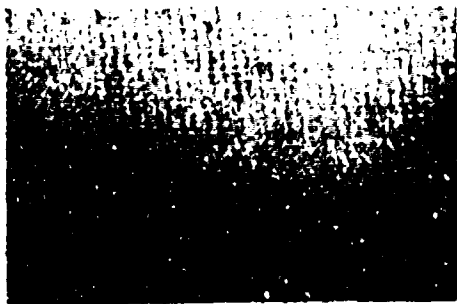
1/64 sec before impact
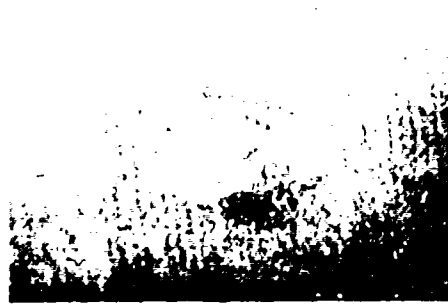
20 sec after impact

impact

40 sec after impact

1/64 sec after impact

60 sec after impact

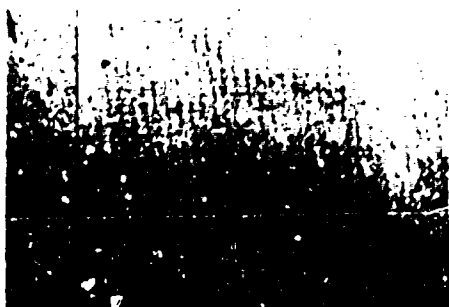FIGURE 14. IMPACT OF STEEL SPHERE AGAINST NATURAL RUBBER
SHEET HAVING GRID IMPRINTED IN A
VAPOR DEPOSIT OF ALUMINUM

79.

to the frequency-to-voltage conversion scheme being used. The compensating amplifier is included because the frequency change will be a linear function of the square root of the distance between the plates.

Unfortunately, by the time the feasibility of this technique for measuring the recovery time of a rubber sheet or coating after an impact has occurred against it was ascertained, time was no longer available to use it to measure recovery time for a series of specific rubbers. Because the recovery time of a rubbery radome coating may be an important property as far as its rain-erosion resistance is concerned, the work of using this electrical technique to measure the recovery times of specific rubbers is proposed as a topic for continuation research (see Section 7).

## 4. CORRESPONDING VELOCITIES FOR EQUAL PRESSURE

The pressures that are transmitted through polyurethane coatings of different kinds as a consequence of Nylon sphere impacts at about 55 ft/sec have been measured [2]. From the standpoint of determining whether rain impingement at 500 mi/hr (733 ft/sec) produces a pressure at the substrate beneath a polyurethane coating that exceeds the crushing strength of the glass fibers and cast resin in a glass fabric reinforced laminate, it is of interest to determine the correspondence between the pressure generated by a Nylon sphere impact at 55 ft/sec and the pressure generated by a waterdrop impact at 733 ft/sec.

### 4.1 THEORETICAL DETERMINATION OF CORRESPONDING VELOCITIES FOR EQUAL PRESSURE IN LIQUID-SPHERE AND SOLID-SPHERE IMPACTS

Impact between a moving target plate and a stationary liquid drop has been idealized [8] as the simple case of collision of two rods with flat ends. That is, if a plate is fired against a drop, a core of material extending through the plate under the contact area is slowed down with respect to the remainder of the plate and a similar core of material through the drop is set in motion. The cores were regarded as true cylinders free to move in the collision direction but restrained laterally.

It was shown by Frankland [8] that plane wave theory can be applied to this case if the plane wave speed of sound (rod speed) given by $(E/\rho)^{1/2}$, where $E$ is the elastic modulus and $\rho$ is density, is replaced by the speed of sound in infinite medium (bulk speed) given by $(E/\rho)^{1/2} \left[ (1-\nu)/(1-2\nu)(1+\nu) \right]^{1/2}$ where $\nu$ is Poisson's ratio. Liquids have only one sound speed.

During collision between a solid Rod A having flat ends and moving with velocity $V$ in a stationary coordinate system and a liquid Rod B that is at rest, there is a radial flow of liquid at the impacted end of Rod B. In order that the rods remain in contact while the compressional waves move through them, the

80.

interface velocity (I) must obey the inequality $V - v' > v$ where $v$, $v'$ are the particle velocities in the compressed zones [9].

One can write $\alpha(V - v') = v$ where $\alpha$ is a dimensionless coefficient having a value less than unity [9]. Then

$$v + \alpha v' = \alpha V. \tag{4.1}$$

Using the relation that exists between stress and particle velocity for plane waves, the equality of stresses at the surface of contact is given by

$$z v = z' v' \tag{4.2}$$

where $z$ is acoustic impedance (product of sound speed and density). From Eqs. (4.1) and (4.2), the particle velocities $v$, $v'$ are found to be [9]

$$v = \alpha z' V / (z' + \alpha z) \tag{4.3}$$

$$v' = \alpha z V / (z' + \alpha z) \tag{4.4}$$

and the plane wave stress for the liquid-solid collision is [9]

$$\sigma_{LS} = \alpha z z' V / (z' + \alpha z). \tag{4.5}$$

The elastic plane wave stress for impact of two solid rods with flat ends (solid-solid collision) is given by

$$\sigma_{SS} = z z' V / (z' + z). \tag{4.6}$$

To obtain equal pressure for a waterdrop impact and a Nylon ball impact against a planar solid having acoustic impedance $z'$, the velocities at which the impacts occur

must be different.  Equating the stresses given by Eqs. (4.5) and (4.6), one finds that

$$V_W = (z_s/\alpha z_w) \left[(z' + \alpha z_w) / (z' + z_s)\right] V_S \qquad (4.7)$$

where $V_W$ is the impact velocity of the water sphere, $V_S$ is the impact velocity of the solid sphere, $z_s$ is the acoustic impedance of the solid sphere, and $z'$ is the acoustic impedance of the planar solid.  The acoustic impedance of solids in this application must be calculated with use of the infinite medium sound speed.  For water, the value of the coefficient $\alpha$ has been found [9] to be 0.4.

If the solid sphere consists of Nylon,

$$V_W = 4.85 \left[(z' + 0.60 \times 10^5) / (z' + 2.91 \times 10^5)\right] V_N \qquad (4.8)$$

where $V_N$ is the impact velocity of the Nylon sphere and the data of Table 6 have been used.  If the planar solid consists of Plexiglas, $V_W = 3.02\ V_N$.  If $V_W$ is 733 ft/sec, $V_N$ is about 244 ft/sec.

It has been hypothesized [10] that for a short time after the first instant of impact a waterdrop cannot flow (no-flow regime).  If this is indeed the case, the coefficient $\alpha$ would be unity in Eq. (4.7) and, for the condition that the solid sphere consists of Nylon,

$$V_W = 1.94 \left[(z' + 1.5 \times 10^5) / (z' + 2.91 \times 10^5)\right] V_N \qquad (4.9)$$

and if the planar solid is Plexiglas, $V_W = 1.49\ V_N$.

It is noteworthy that, regardless of whether the waterdrop flows or does not flow during the initial phase of impact, the corresponding velocities for equal pressure depend on the material of the planar solid that is struck.

82.

## 4.2 EXPERIMENTAL DETERMINATION OF CORRESPONDING VELOCITIES FOR EQUAL PRESSURE IN NYLON-SPHERE IMPACTS AND WATERDROP IMPACTS

Corresponding velocities for equal pressure can be established experimentally by determining what velocity a Nylon sphere must have and what velocity a waterdrop must have to produce equal damage in a given material. An interfering circumstance is that the impact of a waterdrop produces damage both by the pressure that it generates and by the stresses that are associated with the radial flow of the drop liquid.

There is a gas gun at the British Royal Aircraft Establishment in Farnborough, Hants, England, that can fire 5/16-inch-diameter solid specimens against waterdrops at high velocities. Firings of a specified solid material against waterdrops with use of this gun over a series of velocities were offered by Mr. Andrew A. Fyall. The small gas gun that was used in making laboratory tests (see Section 2.4) is available to fire Nylon spheres over a range of velocities.

The material chosen for the experiment was Plexiglas sheet in 1/2-inch thickness. One-inch-diameter circular specimens of this material were inserted in the specimen holder of the small gas gun that was used to make the laboratory tests and 3/16-inch Nylon spheres were fired against them. It was found that no damage at all was done to the Plexiglas even at impact velocities that were close to 1,000 ft/sec.

In the light of this finding, it was necessary to change to a different geometry. The 1/2-inch-thick sheet was replaced by 1/8-inch-thick sheet and 1-inch-diameter circular specimens of this sheet material were placed over a 1-inch-diameter steel backing plate that contained a 5/16-inch-diameter hole at its center. A 3/16-inch Nylon sphere was fired so as to impinge at the center of the 5/16-inch hole in the backing plate. With this geometry, the 1/8-inch-thick Plexiglas sheet flexed over a 5/16-inch-diameter circle. At a compressed air pressure of about 50 psi, which accelerates the Nylon sphere to a velocity of about
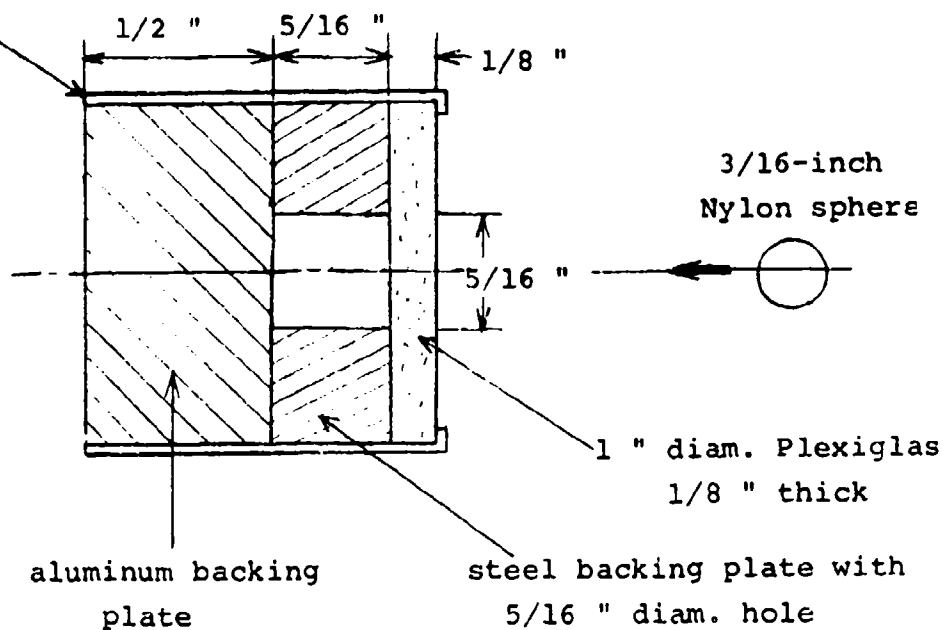
500 ft/sec, a star of cracks formed in the Plexiglas sheet. The
geometry of the arrangement is shown in Figure 15 along with a
picture of the star-shaped crack.

With use of this arrangement, firings with Nylon spheres
were made at progressively lower compressed air pressures until
an air pressure was reached below which the Plexiglas plate did
not flex enough under the impact of the Nylon sphere to produce
crack formation. The threshhold compressed air pressure was
found to be in a range from 16 to 21 psi. At this low pressure
usually only one crack formed in place of a star-shaped cluster.
Strangely, at the pressure of 16 psi two intersecting cracks
formed so that four cracks radiated from a central point. This
suggested that the relative number of imperfections that exist
in the immediate vicinity of the impact site may affect the num-
ber of cracks that form.

The Nylon sphere velocities corresponding to these air
pressures were determined with use of the laser light-ladder
screens. Four firings were made at each pressure; the average
of the four velocities obtained is given in Table 7. No correc-
tion was made for air drag because the distance from the gun
muzzle to the Plexiglas sheet was just half of the light screen
separation distance.

### TABLE 7
#### IMPACT DATA FOR FIRINGS AGAINST PLEXIGLAS

| Air Pressure psi | Impact Velocity ft/sec | Peak Pressure for Average Gas Pressure psi | Ball Contact Area, $A_b$ inch$^2$ | Area Ratio $A/A_b$ -- | Maximum Pressure psi |
|---|---|---|---|---|---|
| 16 | 252 | 2,000 | 0.00785 | 2.56 | 7,621 |
| 17 | 258 | 2,020 | 0.00801 | 2.51 | 7,697 |
| 20 | 293 | 2,420 | -- | -- | 9,215 |
| 21 | 302 | -- | -- | -- | -- |

specimen holder assembly

1/2 "   5/16 "   1/8 "

3/16-inch
Nylon sphere

5/16 "

1 " diam. Plexiglas
1/8 " thick

aluminum backing
plate

steel backing plate with
5/16 " diam. hole

A. GEOMETRY USED TO PRODUCE FLEXURE IN PLEXIGLAS SHEET



5/16 "
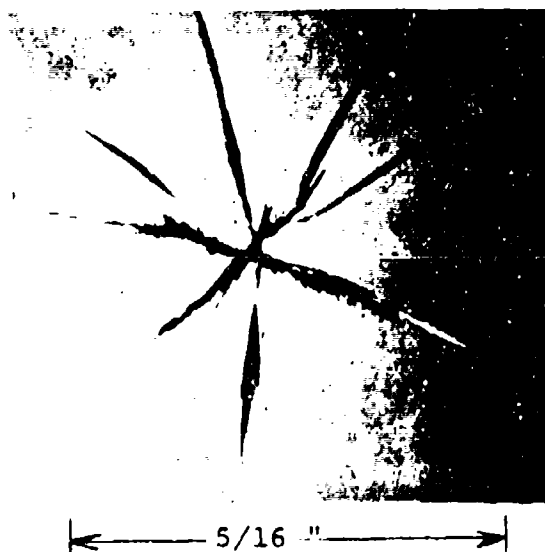
B. MAGNIFIED VIEW OF STAR CRACK FORMED

FIGURE 15. CRACK PRODUCTION UNDER FLEXURE PRODUCED BY
NYLON-SPHERE IMPACT

The pressure transmitted through the Plexiglas sheet was determined with use of the piezoelectric pressure gauge. The Nylon sphere was fired with a gas pressure of 18.5 psi which is the average over the range from 16 to 21 psi. The distance from the gun muzzle to the Plexiglas sheet was 0.5 inch. The measured peak pressure was converted to maximum pressure; to do this, it was necessary to determine the ball contact area $A_b$ between the Nylon sphere and the Plexiglas plate. The data obtained are given in Table 7.

The pressure at the impact surface is a little higher than the transmitted pressure because some loss in pressure occurs as a consequence of passage of the pressure pulse through the thickness of the Plexiglas sheet. The loss in pressure could have been determined by making firings at the same gas pressure using Plexiglas sheets of slightly different thickness but time was not available for the purpose.

The large values of ball contact area, $A_b$, are at first surprising. They result in a low ratio (about 2.5) of quartz crystal area, A, to ball contact area, $A_b$. This ratio for aluminum and stainless steel, when determined at the "standard" velocity of about 55 ft/sec, is 16. The explanation appears to be that at impact velocities of from 250 to 300 ft/sec the Nylon ball undergoes a marked flattening which results in an abnormally large ball contact area and in a much lower maximum pressure (because maximum pressure is peak pressure multiplied by the factor $(3/2)(A/A_b)$ ) than would be expected on the basis of the impact velocity.

Ring cracks that form around a localized pressure are a characteristic mode of failure of Plexiglas which differs from Perspex in that it is brittle. The ring cracks form as a consequence of radial tensile stresses around a localized pressure. According to the Hertz theory of impact of balls, these tensile stresses, $\sigma_r$, are given by $(1 - 2\nu)(q_0/3)$ where $\nu$ is Poisson's ratio and $q_0$ is the maximum pressure. From Table 7, the average value of $q_0$ is 8,167 psi. If $\nu$ is taken to be about 0.3 then $\sigma_r$ is less than 1,000 psi. This is only about one sixth

of the lowest values of tensile strength given [11] for Plexiglas. Consequently, formation of ring cracks would not be expected and none were observed.

The flexural strength of Plexiglas is almost double the tensile strength [11]. Nevertheless, crack formation due to flexing of the Plexiglas plate of 1/8-inch thickness was observed. The presumption is that the extent to which the 3/16-inch Nylon sphere flattens is less important for the case that a 5/16-inch-diameter circular plate of Plexiglas sheet is flexed than for the case that radial tensile stresses form around the localized impact pressure.

Several small sheets cut from the same 1/8-inch-thick Plexiglas sheet material were sent to Mr. Andrew A. Fyall for an attempt to determine the waterdrop impact velocity that would correspond to the Nylon-sphere velocity that has been determined. The gun used to accelerate specimens of solids against waterdrops cannot accomodate a plate size larger than 5/16 inch and the waterdrop against which it is fired cannot be much larger than 0.1182 inch (3 mm).

To establish a waterdrop velocity that can be compared with the Nylon-sphere velocity that has been determined, the ratio of drop diameter to the diameter of the area over which flexure occurs should be the same. For the Nylon-sphere velocity determination described above this ratio is (3/16)/(5/16) or 0.6. If a 0.1182 inch drop is employed in the corresponding waterdrop velocity determination, a supporting ring that has an inside diameter of 0.197 inch should be inserted under the Plexiglas sheet. The drop impact should occur in the center of the area that is free to flex.

What will be discovered when the waterdrop impact study is carried out will be reported separately by Mr. Fyall at Royal Aircraft Establishment. It is noteworthy that waterdrops do not tend to flatten during impact (at least not during the first stage of impact) and the formation of ring cracks as a result of waterdrop impacts against Plexiglas is to be expected. In fact, circles of cracks as the result of waterdrop impacts against

87.

Plexiglas have been observed in a specimen of poly(methyl methacrylate) (Lucite) that was tested on a rotating-arm device for a very short period of time [12]. If ring cracks occur as a result of waterdrop impacts against Plexiglas before cracks form as a result of flexing, the attempt to determine corresponding velocities for equal fracture with use of Plexiglas will be unsuccessful. It is necessary that the fracture mechanism be the same for the waterdrop impact and the Nylon ball impact. Perhaps crater formation in a soft material would have been a better way to establish corresponding velocities than crack formation in Plexiglas.

## 5. TESTING METHODS FOR RAIN-EROSION RESISTANCE

The study of composite coatings that has been carried out [1,2,3] has been hampered by the finding that stresses, which are inherent in the rotating-arm test device but which do not exist on a radome, can reverse the relative rain-erosion resistance rating of a series of candidate radome coatings. These irrelevant stresses are primarily centrifugal force, which is inherent in all rotating devices, and internal stresses that are a consequence of specimen shape and the use of restraining frames and clips.

Centrifugal force stretches a rubbery coating specimen from its low-speed to its high-speed end. The specimen is tested, as it were, while under tension. In this stressed state it is subjected to the vibration generated by the rotating arm. In addition, the accumulated liquid from drops that have already impinged is driven at high speed over the surface of the specimen by centrifugal force.

It has been pointed out [2] that the curved shape of an airfoil test specimen results in unequal yield along the shoulder of the specimen. This is because a drop that impinges at the center of the leading edge sees a coating which has support immediately below it but a drop that impinges at a substantial distance to either side of the center of the leading edge sees a coating that is supported from the side. The same kind of unequal yield occurs along a restraining frame; this is because the coating that is under the restraining frame does not yield as a consequence of the drop impacts that occur against the frame but the coating material that is not protected by the frame does yield.

The result of unequal yield is the generation of cracks that grow in length. These cracks result in the loss of material at the surface of the coating not only because they are hit by additional drops but also because the high-speed flow of accumulated drop liquid, which is driven by centrifugal force,

bears against them. Some coatings are more subject to genera-
tion of fatigue cracks as a consequence of unequal yield than
other coatings. Such candidate radome coatings, if tested in
the presence of unequal yield, would be eliminated as having
poor rain-erosion resistance. However, the fact remains that
neither unequal yield nor centrifugal force is encountered on a
radome.

These considerations prompt action in (1) eliminating ir-
relevant stresses from the rotating-arm device and/or (2) de-
vising new test methods or procedures that are not subject to
the irrelevant stresses. With regard to action (1), airfoil
shaped test specimens can be replaced by flat specimens. This
step was taken in carrying out the rain-erosion tests for the
study described in this report. However, unequal yield along
the restraining frame is then encountered. It is possible that
the unequal yield along the restraining frame can be mitigated
if not overcome by cutting the coating away along the edge of
the specimen so that the restraining frame will bear against
the coating substrate rather than against the coating. With
regard to action (2), some progress has already been made.

## 5.1 Flight Tests

Flight tests were among the earliest test procedures that
were explored. Flight tests of Lucite plastics and of a number
of different coating materials were reported by Lapp, Stutzman,
and Wahl [13] in 1955. For these tests, specimens of various coat-
ings were applied directly to the metal leading edge of an air-
plane that was secured for the purpose. Coatings were also ap-
plied to glass reinforced laminates that were bonded to the
leading edge of the airplane. Each material was tested with
duplicate specimens; one specimen was applied to each wing of
the airplane. The test time for specimens in the flight tests
was an accumulation of small increments of time in flight
through natural rains of different intensities (described as
moderate to light rain, fairly light rain, extremely light rain,
and a heavy thunderstorm).

From the standpoint of real conditions, flight tests probably provide the best way to test candidate radome materials for rain-erosion resistance. The possibility of mounting a small panel containing specimens of coating materials on a commercial airplane for exposure to weather and to high-speed rain impact was taken up with Mr. Henry Harrison, Manager of Avionics Engineering, Eastern Airlines, Miami, Fla. Mr. Harrison suggested that it might be possible to mount a small panel containing coating specimens with use of an epoxy adhesive to the leading surface of the tail stabilizer of a commercial airplane. This structure is subject to rain impingement; it is usually left unpainted because paints are eroded away.

The attractive feature of this method of test is that all the coatings on a specific panel would be subjected to the same weathering conditions as well as to the same rain impingement conditions as the airplane makes the flights to which it is assigned. The unattractive feature is that it is the policy of commercial airlines either to avoid flying in rain or to fly through it at low speed. At best, the test would indicate the relative rain-erosion and weathering resistance of coatings under commercial flight conditions.

Mounting test specimens on the research airplanes that fly into storms and hurricanes might provide a better test than mounting them on a commercial airliner. It was learned from Mr. Richard Decker of Research Flight Division of National Oceanic and Atmospheric Administration that two airplanes are available in Miami, Fla. These are a DC-6 and a C-130 each of which cruises at about 250 mi/hr. It is possible that coating specimens could be mounted on one of these research airplanes for flights into hurricanes in October this year. For flights at higher speeds, a Convair 990 research airplane, which flies at 500 to 600 mi/hr, is available at NASA Ames Research Center. Flights on this plane can be arranged through Dr. Peter Kuhn of National Oceanic and Atmospheric Administration in Boulder, Colo.

91.

Flight tests were carried out recently at Singapore by Mr. Andrew A. Fyall and Mr. Roy B. King of Royal Aircraft Establishment at Farnborough, Hants, England. In an informal discussion of this work it was stated that direct correlation with ground tests was difficult because the specimens were mounted over a range of impact angles for different flights and the flights were carried out at different velocities and under different rainfall conditions. However, large areas of the airplane including radomes were coated with polyurethanes. Correlation with expected performance on the basis of ground tests was excellent for the polyurethane coated areas. A report of these tests is in process of preparation.

## 5.2 ACCELERATION OF WATERDROPS AGAINST STATIONARY TEST SPECIMENS

An electrical waterdrop accelerator has been constructed under the direction of Prof. C.D.Hendricks at the University of Illinois, Urbana, Ill. At the present time the device is capable of accelerating very small waterdrops to velocities as high as 30,000 ft/sec. It is capable of producing multiple impacts with 1-mm drops for periods of indefinite length at 500 mi/hr (733 ft/sec). Drops that are 2 mm in diameter can be brought up to close to 500 mi/hr.

This equipment is already being used for a classified project. It will be available for test of candidate radome coating specimens using 1-mm drops at 500 mi/hr on a continuous multiple impact basis by August or September this year. The cost of making a similar device was estimated at from $100,000 to $200,000 for personnel and equipment.

Some consideration was given to the possibility of accelerating waterdrops by mechanical means and directing them against stationary test specimens. The idea considered was a water channel through a rotor arm which would be operated at reduced pressure. A rotating baffle at the high-speed end of the rotor arm was considered as a means of delivering discrete drops. No attempt was made to construct a mock-up of this device.

92.

## 6. SUMMARY OF CONCLUSIONS

The following conclusions have resulted from the study that has been carried out:

(1)    The rain-erosion resistance of polyurethane coatings is strongly reduced by outdoor weathering for ten weeks.  Although they appear only to have darkened in color, the coatings have little value for rain-erosion protection after this amount of weathering.

(2)    Both the two-layer composite and the single-layer polyurethane coatings are strongly subject to sand erosion when sand impacts occur at normal incidence against flat test specimens.

(3)    The multilayer composite coating has rain-erosion resistance that is either comparable or superior to the rain-erosion resistance of the two-layer composite coating.  This finding suggests that the shear stress exerted by an impinging drop may be relatively unimportant as long as the surface of impingement remains planar.

(4)    Use of a two-layer composite coating may result in a more stable and predictable average rotating-arm test lifetime than use of a single-layer coating.  More test results are needed to demonstrate this conclusively.

(5)    The $S_2$ single-layer soft polyurethane coating may or may not perform as well as the $H_1S_2$ two-layer composite polyurethane coating depending upon the quality of the $S_2$ coating; this finding points to the need for increased quality control in coating preparation and application.

(6)    One mode of hole formation in polyurethane coatings during rain-erosion test can be identified with isolated fatigue cracks that develop in the coatings.  To be rain-erosion resistant a material must resist formation of cracks as a consequence of fatigue in repetitive yielding under random high speed rain impacts.

(7)    Although some reflection of the impact pressure pulse within a coating is beneficial in that it reduces loading rate and the magnitude of the pressure transmitted to the substrate, a threshold may exist beyond which increased reflection is deleterious. The loading rate and transmitted pressure of the stress-bumper coating were higher than those of the two-layer composite coating. The stress-bumper coating lost adhesion during rain-erosion test.

# 7. SUGGESTED TOPICS FOR CONTINUATION RESEARCH

## (1) Effect of Weathering Factors on the Rain-Erosion Resistance of Polyurethane Radome Coatings

One of the most important results of the study described in this report is the finding that the rain-erosion resistance of moisture-cured polyurethane coatings is strongly reduced by outdoor weathering. The seriousness of this finding resides in the fact that although a polyurethane coating on a radome may appear to be in excellent condition several months after it was applied, its rain-erosion resistance may have dwindled to less than a fifth of its freshly-applied value unless some form of protection against weathering deterioration was employed. The finding that polyurethane coatings are strongly subject to weathering deterioration should motivate a study of the factors that are involved in the weathering process and in attempts to by-pass their action.

The effect of the five weathering factors (oxygen, ozone, humidity, temperature, and ultraviolet light) can be monitored by testing specimens that are stored under conditions in which these factors are controlled. One factor should be varied at a time while the others are maintained constant.

Attack by oxygen and ozone may be mitigated by adding anti-oxidants to the polyurethane. Test of the same polyurethane material with and without the addition of antioxidants after a specified period of weathering should provide some insight into the extent to which oxygen and ozone are involved in the weathering deterioration of polyurethane coatings. Ozone may be involved in breaking bonds.

Attack by ultraviolet light may be mitigated by the use of a surface layer that would reflect the violet and ultraviolet wavelengths and so prevent them from passing through the polyurethane material itself. In this connection, a composite coating consisting of a polyurethane undercoat overcoated with a white ceramic topcoat suggests itself. The optimum thickness of the polyurethane layer and ceramic layer would have to be determined by trial.

94.

It is noteworthy that the addition of carbon black to poly-urethane may afford some protection against attack by ultraviolet light. The amount of protection that addition of carbon black does bestow should be determined by tests. Deleterious effects that may result from the use of carbon black should also be assessed.

Work that has already been done shows that polyurethane loses strength as temperature is increased because of the reduction of the Van der Waals forces of attraction between polymer chains. The reaction is reversible and strength is regained as the temperature is reduced.

(2) Measurement of the Recovery Time of Rubbers

The possible effect of recovery time of a rubber on its rain-erosion resistance has been discussed in this report. The importance of recovery time resides in the fact that if an additional drop impact occurs at a point which has not yet recovered from an earlier impact the rubber at that point does not have its full ability to yield and this may possibly result in initiation of failure.

In the study described in this report it was not found possible to measure the recovery time of a rubber coating after impact with use of optical techniques. A feasible electrical method was described but time was not available to assemble apparatus and make measurements of recovery time. It is recommended that the recovery time of rubbery coatings, the rain-erosion resistance of which is known, should be measured by use of this electrical technique and that the effect of recovery time of a rubber on its rain-erosion resistance should be determined.

## 8. REFERENCES

1. Olive G. Engel and Andrew J. Piekutowsky, Final Report, Naval Air Systems Command Contract N00019-71-C0108, Nov. 1971.

2. Olive G. Engel, Final Report, Naval Air Systems Command Contract N00019-72-C-0286, May 1973.

3. Olive G. Engel, A Study of Composite Coatings for Rain-Erosion Protection of Radomes, Fourth International Conference, Rain Erosion and Associated Phenomena, Meersburg, Lake Constance, Federal German Republic, 8-10 May 1974.

4. Norman E. Wahl, Quarterly Progress Report No. 2, Contract AF 33615-73-C-5057, September 1973.

5. Olive G. Engel, Fragmentation of Waterdrops in the Zone Behind an Air Shock, J. Research Nat'l. Bur. Stds. 60, 245 (1958).

6. Chemical Rubber Company Handbook of Tables for Applied Engineering Science, Roy E. Boly and George L. Tuve, editors, Second Edition, 1973.

7. Vapor deposition of was accomplished with apparatus available in the Biology Department and in the Physics Department of Florida Atlantic University.

8. Olive G. Engel, Pits in Metals Caused by Collision with Liquid Drops and Soft Metal Spheres, Nat'l. Bur. Stds J. of Research 62, 229 (1959).

9. Olive G. Engel, Particle Velocity in Collisions Between Liquid Drops and Solids, Nat'l. Bur. Stds. J. of Research, 64A, 497 (1960).

10. F.P.Bowden and J.E.Field, Proc. Royal Society (London) 282 A, 331 (1964).

11. Engineering Manual, Robert H. Perry, editor, McGraw-Hill Book Company, New York, New York, 1967.

12. Olive G. Engel, Mechanism of High-Speed-Waterdrop Erosion of Methyl Methacrylate Plastic, Nat'l. Bur. Stds. J. of Research, 54, 51 (1955).

13. Roy R. Lapp, Raymond H. Stutzmn, and Norman E. Wahl, Wright Air Development Center Technical Report 53-185 Pt. II, 1955.

The impact of a 3/16-inch Nylon sphere at about 55 ft/sec was used as a "standard impact" in laboratory determinations of coating resilience and of pressure transmitted through a coating [1,2]. The velocity of 55 ft/sec was found by trial to be the highest velocity that could be used without producing permanent deformation or set in a 15-mil-thick polyurethane coating as the result of impact of a 3/16-inch Nylon sphere. On this basis it was thought that this velocity for a Nylon sphere may produce about the same impact pressure as that produced by a waterdrop at 500 mi/hr (733 ft/sec). An initial study of the corresponding velocities for equal pressure between Nylon sphere impacts and waterdrop impacts is described in Section 4 of this report.

In the first work that was done on the recovery time of rubbery coatings, the small gas gun that was used to fire Nylon spheres at the University of Dayton Research Institute [1,2] had not yet been received, installed, or brought into operating condition at the Florida Atlantic University. It was necessary to simulate the "standard impact" with use of a freely falling steel sphere. To do this it was necessary to know the fall height that must be used for the sphere.

To establish what the correct fall height of the sphere should be, the corresponding velocity for equal pressure between a Nylon ball impact at 55 ft/sec and a steel sphere impact was calculated. Hertzian equations for impact of a solid sphere against a planar solid are available [2]. The pressure $P_N$ developed when a Nylon sphere impinges against a planar solid having elastic modulus $E'$ is given by

$$P_N = 0.9025 \left[ (E_N E')^4 \, \rho_N v_N^2 \, / \, (E_N + E')^4 \right]^{1/5} \tag{3.1}$$

where $E_N$ is the elastic modulus of Nylon, $\rho_N$ is the density of Nylon, and $v_N$ is the impact velocity of the Nylon sphere.

66.